IEM JOURNAL

THE JOURNAL OF THE INSTITUTION OF ENGINEERS, MALAYSIA
KDN PP5476/10/2012 (030203) | ISSN 0126-513X

The Institution of Engineers, Malaysia

VOL. 85, NO. 2
DECEMBER 2024

Vol. 85, No. 2, December 2024
KDN PP5476/10/2012 (030203) ISSN 0126-513X

CONTENTS

THIS ISSUE WAS PUBLISHED IN NOVEMBER 2024

For advertisement placements and subscriptions, please contact:
DIMENSION PUBLISHING SDN. BHD. (449732-T)
Level 18-01, PJX-HM Shah Tower, No.16A, Persiaran Barat, 46050 Petaling Jaya, Selangor Darul Ehsan, Malaysia.
Tel: +(603) 7493 1049 Fax: +(603) 7493 1047
E-mail: info@dimensionpublishing.com

Printed by
DIMENSION PUBLISHING SDN. BHD. (449732-T)

PRINT QUANTITY: *500 COPIES*

IEM Journal
June 2024 Vol. 85, No. 1
Visit the IEM Journal website at
https://iemjournal.com.my/index.php/iem
or scan the QR code to read online

MODELLING OF WATER QUALITY PARAMETERS OF LOWER USUMA DAM RESERVOIR, ABUJA, USING ARTIFICIAL NEURAL NETWORK (ANN)

Haruna Garba[1*] and Francis Peter[2]

Abstract

The water quality parameters of Lower Usuma Dam, Abuja, were analysed and modelled using an artificial neural network (ANN). Monthly water quality parameters of pH, turbidity, electrical conductivity, total dissolved solids, and total hardness for a duration of 6 years (2017–2021) were obtained from the Water Laboratory Department of the Federal Capital Territory of Nigeria (F.C.T.) Water Board, Abuja. Microsoft Excel was used to analyse the trends of these parameters. The Artificial Neural Network (ANN) was used to develop three model equations for the prediction of electrical conductivity, total dissolved solids, and total hardness, respectively, with pH and turbidity as input parameters. F-tests and t-tests were used to validate each model using Microsoft Excel. The error analysis and performance evaluation of the applied models were also done to evaluate the goodness and suitability of each of the models. The coefficients of determination (R2) between the parameters were 0.89085, 0.83156, and 0.86931 for testing, training, and validation, respectively. A very strong relationship between the predictors (pH and turbidity) and the response variables (electrical conductivity, total dissolved solids, and total hardness) was established. The root mean square errors were 11.2, 13.8, and 5.54. Thus, the total hardness model is the best among them because it has the lowest predictive error. The model validation carried out for the F-test and t-test for electrical conductivity, total dissolved solids, and total hardness, respectively, shows that F critical is greater than F, as well as t critical is greater than t-stat. This further shows that the ANN model is fit for the prediction of water quality.

Received: *21 February, 2024*
Revised: *11 June, 2024*
Accepted: *15 August, 2024*

*[1,2]Department of Civil Engineering,
Nigerian Defence Academy,
PMB 2109 Kaduna, Nigeria.*

***Corresponding author:**
hgarba@nda.edu.ng

Keywords:
Artificial neural network, Dam, Modelling, Parameters, Water quality

1.0 INTRODUCTION

All living things depend on water as a vital natural resource for survival. Water is mostly needed by humans for domestic, industrial, and agricultural purposes (Ehya and Saeedi, 2019). According to current data on water consumption worldwide, ten percent (10%) of available fresh water is used for home purposes (drinking, cooking, bathing, etc.), seventy percent (70%) is used for agriculture, mostly irrigation, and twenty percent (20%) is used for industrial purposes (Boretti and Rosa, 2019). According to Boretti and Rosa (2019), domestic, agricultural, and industrial purposes are expected to increase dramatically in the years to come. By 2050, there will likely be a 20–30% increase in the demand for water for a variety of uses. The human population is rapidly increasing around the world. Hence, there is an increased need for clean water to carry out human activities. Even though there is a greater need for water, there is less freshwater available because of pollution and fewer sources. Contaminated water resources have negative health effects and have a significant negative impact on both the environment and overall human wellbeing; ensuring water quality for domestic, drinking, and agricultural purposes is crucial and desirable (Egbueri *et al.,* 2019). According to Mrunmayee (2014), contamination of surface water by chemical, physical, and microbiological contaminants is a global epidemic. The physical, chemical, microbial, and biological conditions in the water courses and subsurface aquifers have an impact on fish survival and growth, biodiversity, conservation efforts, leisure activities like swimming and boating, industrial and municipal water supply, agricultural uses like irrigation and livestock watering, waste disposal, and all other water uses (Singh *et al.,* 2005).

In 2021, Marian *et al.* (2021) explore the use of ANN to predict the monthly values of dissolved oxygen (DO) and electrical conductivity (EC) to analyse the water quality parameters of four variables and discharges. The correlation coefficient, root-mean-square error, and mean absolute error were the statistical criteria explored for evaluating the model's performance. The potential of ANN for simulating relevance between water quality parameters indicates that ANN can discern the pattern of water quality to offer an appropriate prediction of changes in water quality data. In forecasting water parameters, use ANN for irrigation purposes. Uba *et al.* (2021) analysed the water quality index of four parameters [PH, Total Dissolved Solids (TDS), Electrical Conductivity (EC), and Sodium (Na) of the Ele river at different locations using ANN. Results from the analysis showed that the PH ranged from 6.01 to 6.87, while the TDS ranged from 3.01 to 5.76 and 40.42 to 73.45, respectively. Findings from the study showed that the R2 values range from 0.956 to 0.967, 0.953 to 0.970, 0.951 to 0.967, and 0.953 to 0.968 for each of pH, TDS, EC, and Na, while the forecast performance evaluation showed R^2 values of 0,022 to 0.088, 0.12 to 0.087, 0.015 to 0.085, and 0.014 to 0.084.

The efficiency of hybrid deep neural networks and the multivariate water quality forecasting model in the aquaculture ecosystem was examined by Elias *et al.* (2023) by developing a novel hybrid deep learning neural network multivariate water quality parameters forecasting model with the aid of the ensemble empirical mode decomposition (EEMD) method, deep learning long-short term memory (LSTM), neural network (NN), and multivariate linear regression (MLR) method. The performance of the novel hybrid water quality forecasting model is validated by comparing the forecasted results with water quality parameter data. The forecast accuracy of the result suggested that the novel hybrid water quality forecasting model can be used as a valuable support tool for water quality management in aquaculture industries.

An efficient river water quality indicator prediction model was designed and built by Jitha in 2023. Data were collected from eleven sampling stations at different points on the Bhavani River in Kerala and Tamil Nadu, India. The water quality index was computed using twenty-eight different parameters that affect water quality. Feature selection and data normalization are applied to develop an efficient river water quality database. The water quality index (WQI) prediction model was built using deep learning architectures. The performance of the deep learning-based WQI prediction model is compared with that of traditional learning-based models. The performance analysis indicates that the GRU-based prediction model shows promising results in predicting water quality.

A simple architecture consisting of an artificial neural network model for water quality and water consumption prediction was proposed by Furaun *et al.* (2022). An artificial neural network (ANN) consisting of one hidden layer and a couple of dropout and activation layers is utilised. The approach is tested using two data sets for predicting water quality and water consumption. Results show a 0.96 accuracy for water quality prediction. A 0.99 score is obtained for water consumption prediction.

The cost of labour and materials for many chemical tests, as observed by Mrunmayee (2014), can be somewhat reduced by using water quality models as effective tools to forecast and simulate contaminant transport in aquatic environments. The aim of this research work, therefore, is to leverage the application of ANN as a cost-effective means and approach for analysing and predicting water quality parameters. The ANN tool was used to develop model equations for the prediction of electrical conductivity, total dissolved solids, and total hardness for the Lower Usuma Dam reservoir. Though ANNs have been extensively used in modelling various environmental parameters, including water quality parameters, however, they come with their own set of limitations in the following contexts: complexity requirements, complexity and interpretability, sensitivity of input data, and limited transferability. To address these limitations and pave the way for future research into using ANNs for modelling water quality parameters, the following suggestions can be considered: Integration with other models, Data quality improvement, integration techniques, Feature selection and dimensionality reduction, Models explain ability.

2.0 MATERIALS AND METHODS

2.1 Description of Study Area

The lower Usuma dam is located at latitude 7o 25' 16" east and longitude 9o 01' 12" north. The dam is constructed across the River Usuma and is situated 10 kilometres from Bwari and 26 kilometres from the heart of Abuja city (Figure 1).The lower Usuma dam has an installed capacity of about 120 million m3 of untreated, raw water in its reservoir. The main dam and the saddle dam are the two sides of the dam. The main dam embankment is 10 meters in height, 1.3 kilometres long, and 47 meters high, while the saddle dam is 470 meters long, 15 meters high, and 10 meters wide. The dam occupies a total area of 2,500,000 m^2.

Figure 1: Location map of Lower Usuma Dam treatment plant

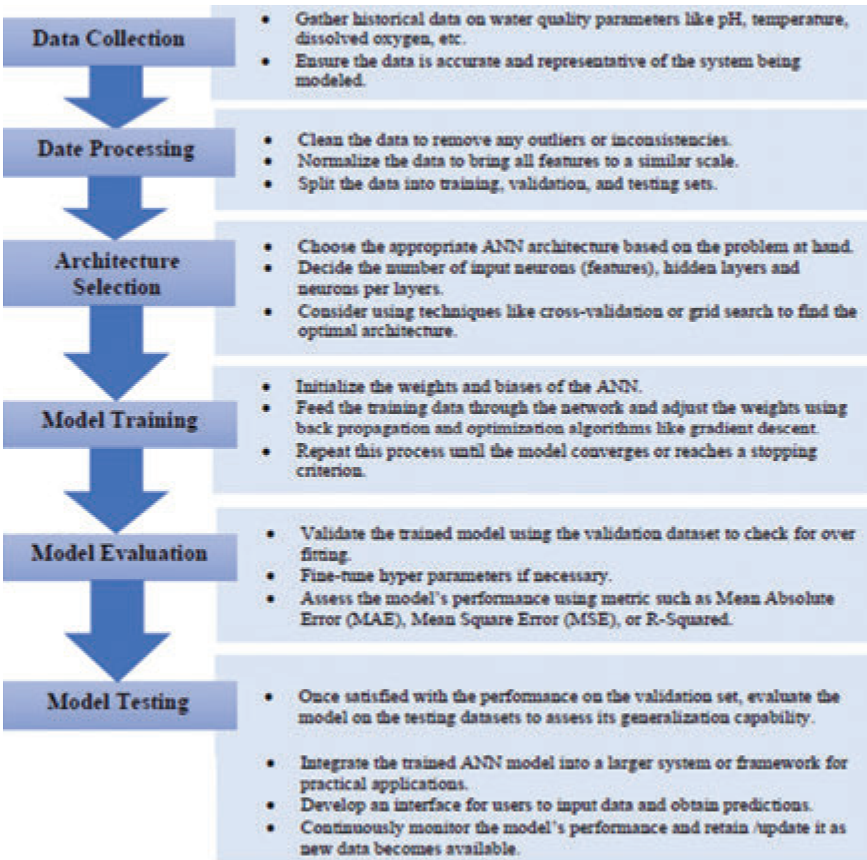

Figure 2: Flow chart of methodology used in the study

2.2 Data Collection

The monthly water quality samples were collected and analysed for the months of January to December from 2017 to 2021. Five physical and chemical water quality parameters were selected for the analysis. The parameters were pH, turbidity, electrical conductivity, total dissolved solids, and total hardness as $CaCO_3$. The flow chart methodology used in the study is presented in Figure 2.

2.3 Method of Analysis

Spearman's correlation analysis, trend analysis, and summary statistics were used to investigate the temporal and spatial variations and to interpret the large and complex water quality data sets that were collected. The data set was divided into three, namely, training, testing, and validation data sets (Nguyen *et al.,* 2018). The Spearman's rank correlation coefficient was estimated temporally for each parameter from 2017 to 2021 to know the positive and negative trends.

2.4 Tools for Analysis

The most effective learning method for multilayer neural network topologies was the back propagation algorithm. The feed-forward-back propagation neural network (BPNN) always has three layers: an input layer, a hidden layer, and an output layer (Figure 3). Before analysing fresh data for the following process, a network first needs to be trained. The neurons in each layer, known as layers, were connected to one another by weights (Figure 3); these neurons were known as neurons in the input layer, which delivered their output to neurons in the hidden layer as input, and similar connections existed between the hidden and output layers. Depending on the issue at hand, the number of hidden layers and the density of their neurons were altered. As with input and output variables, there were an equal number of input and output neurons, (ASCE Task Committee, 2000).

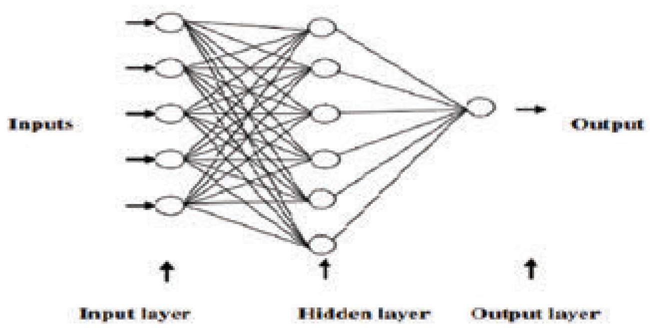

Figure 3: Structure of a multi-layer feed forward artificial neural network model

Values known as biases (Figure 4) were introduced in the transfer functions and were referred to as the temperature of a neuron in order to distinguish between the various processing units. The transfer function filtered the summed signals that were received from this neuron, but the bias behaved like a weight and had an input of 1 (Figure 3). The transfer functions were straightforward step functions, either linear or non-linear, that were intended to convert neurons' or layers' net output to their actual output. All the neurons in the BPNN were connected to a bias neuron and a transfer function, except for the input layer. Transfer function use was dependent on the neural network's intended use. The output layer was created, and the solution-related vectors were calculated (Archana and Prashant, 2015).

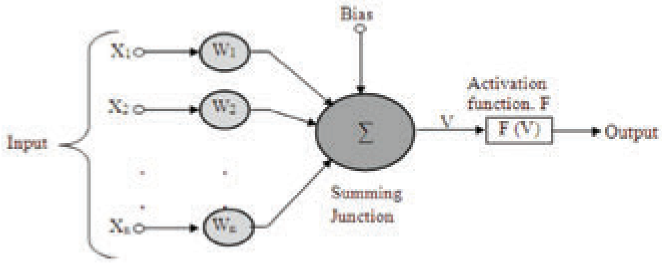

Figure 4: Basic elements of Artificial Neuron

Similarly, the architecture of the ANN model, which uses the non-associated flow rule for its analysis, consists of ten (10) neurons in the hidden layer, three (3) neurons in the output layer, and two (2) neurons in the input layer. Furthermore, the tan-sigmoid function was used as the nonlinear activation function (transfer function) for the hidden layer, while for the output layer, a pure linear function was used as the activation function. The feed-forward neural network trained by the back propagation algorithm was used (Ali, *et al,* 2009).

In this work, two approaches for selecting data were used to build and evaluate the models. In the first approach, the water quality data were divided into two sets. The first set contained 70% of the records and was used as a training set; the second set contained 30% of the records and was used as an over fitting test (Roza and Mohsen, 2021), with 15% for validation and 15% for testing. The training set is used to train the model, and the validation set is used to tune hyper parameters to prevent overfitting. An ANN architecture (feed-forward neuron network) was considered appropriate and used for the study. The number of input neurons (features), hidden layers, and the number of neurons in each layer were determined. Four input neurons corresponding to the number of water quality parameters were used.

2.4.1 Performance Evaluation

There are numerous statistical metrics that can be used to evaluate the suitability or goodness of any given model. In the current study, root-mean-square error (RMSE), coefficient of correlation (R), and coefficient of determination (R^2) performance evaluation statistics were used for ANN training. The (R^2) values were calculated analytically by calculating the square of the correlation coefficient (R), whilst the RMSE and R values were taken from the ANN (Thair and Abdul, 2014). The RMSE is calculated using Equation 1.

$$\text{RMSE} = \sqrt{\frac{1}{n}\sum_{i=1}^{n}(y_i - \hat{y}_i)^2} \quad (1)$$

Where n is the number of observations of the data points, represent the actual n values of observations and represent the predicted or estimated values of observations. Microsoft Excel was used to carry out F- and T-tests for model validation and plot line charts in order to analyse the trend of each of the water quality parameters over time. The monthly water quality parameters (pH, turbidity, electrical conductivity, total dissolved solids, and total hardness), obtained from the F.C.T. Water Board, Abuja, were used for the model validation. Both the measured and the ANN-predicted outcomes for each water quality parameter mentioned above were used for the validation of the electrical conductivity, total dissolved solids, and total hardness models; pH and turbidity were used as input parameters. The t-test and F-test are two commonly used statistical methods in hypothesis testing and analysis of variance (ANOVA). The t-test is used to determine if there is a significant difference between the means of the observed and predicted values of model parameters. The significance of the test provides insight into whether the difference observed between the modelled and predicted parameters is likely due to chance variation or is statistically significant. The F-test, on the other hand, is used in the analysis of variance to compare the variance between the two groups. It is significant in determining whether the differences between multiple groups are due to actual differences between the groups, or could occur due to chance.

3.0 RESULTS AND DISCUSSIONS

3.1 Water Quality Parameters

The descriptive statistics and summary statistics for each of the five (5) raw water quality parameters under consideration were carried out using Microsoft Excel, as well as the various line charts showing data trends for each of the parameters from 2017 to 2022. These results are shown in Figure 5. A summary of the mean, standard error, median, standard deviation, and sample variance is presented in Table 1.

The analysis of the pH shows a range of 6.45–9.61, which is slightly above that of the Nigeria Standard for Drinking Water Quality (NSDWQ) range of 6.5–8.5. The lowest and highest values were recorded in December 2017 and February 2022, respectively, as shown in Figure 5 and Table 1. However, the mean pH value is 7.00.

The turbidity is within the range of 1.6–36.21 NTU, which is by far higher than the NSDWQ standard of 5.0 NTU. The mean value of turbidity is 7.11. The lowest and highest values were recorded in January/February 2017 and October 2022, respectively, as shown in Figure 5 and Table 1.

The electrical conductivity falls within the range of 16.8–89.9 µS/cm, which is within the NSDWQ acceptable limit of 1000 µS/cm. The lowest and highest values were recorded in November 2019 and April 2019, respectively, as shown in Figure 5 and Table 1. However, the mean EC value is 74.35 µS/cm.

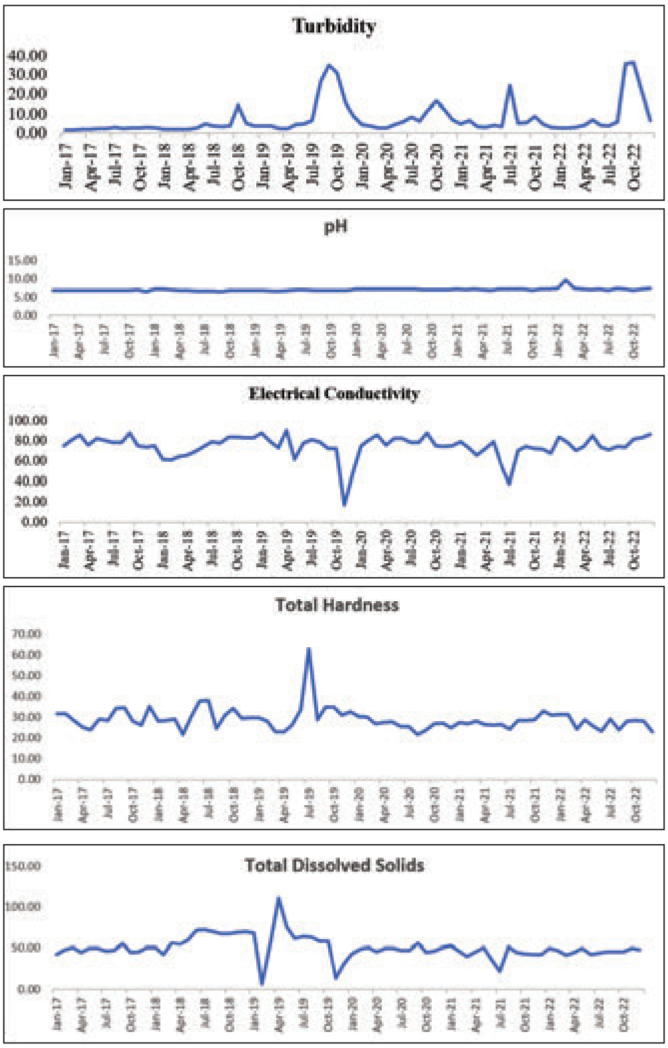

Figure 5: Line chart showing turbidity, pH, electrical conductivity, total hardness and total dissolved solids

The total dissolved solids (TDS) fall within the range of 6.5–110.7 mg/l and are within the NSDWQ permissible limit of 500 mg/l. The lowest and highest values were recorded in February 2019 and April 2019, respectively, as shown in Figure 4 and Table 6. However, the mean dissolved solid TDS value is 50.68 mg/l.

The total hardness is within a range of 21.5–63.0 mg/l and is within the NSDQW permissible limit of 150 mg/l. The lowest and highest values were recorded in August 2020 and July 2019, respectively, as shown in Figure 7 and Table 5. However, the mean total hardness value is 28.91 mg/l.

Table 1: Summary statistics of pH, turbidity, electrical conductivity, total hardness and total dissolved solids

Mean	Standard Error	Median	Mode	Standard Deviation	Sample Variance	Minimum	Maximum
7.0039	0.0432	7	6.9	0.3668	0.1346	6.45	9.61
7.1069	0.9832	3.85	2.7	8.3430	69.6067	1.62	36.21
74.3496	1.3177	75.05	78.2	11.1808	125.0111	16.8	89.9
50.6786	1.6483	49.155	44.9	13.9863	195.6188	6.5	110.7
28.9095	0.6468	28.38	28.9	5.4883	30.1222	21.5	63

3.2 Artificial Neural Analysis (ANN) Analysis

Water quality indicators (electrical conductivity, total dissolved solids, and total hardness) were modelled using the ANN model, and the Feed Forward Multilayer Perceptron (FFMLP), which is a learning algorithm and a feed forward neural network as described earlier, was executed in MATLAB (R2016a).

The ANN model performed excellently in both the training, testing, and validation data sets, based on the R (correlation coefficient) and R^2 (coefficient of determination) values in Table 2. The R values are 0.94385, 0.9119, and 0.93237 for the testing, training, and validation datasets, respectively. Consequently, the R^2 values for the testing, training, and validation datasets are 0.89085, 0.83156, and 0.86931, respectively. This is similar to the result obtained by (Khandelwal and Singh, 2005). A statistical instrument that assesses the strength of the linear relationship between experimental and expected values is the correlation coefficient (R).

The results of the root-mean-square error (RMSE) are displayed in Table 3 and are also consistent with those of the R, showing a close range for all the training, testing, and validation data sets. RMSE revealed that the performance for electrical conductivity and total hardness was lower when compared with total dissolved solids. In other words, the electrical conductivity and total hardness models have the lowest prediction error for the training and validation data sets. The total hardness model is the best among them because it has the lowest RMSE value of 5.54. The ANN model performed very well, as their coefficient of multiple determinations, R^2, was very close to 1, which is in agreement with the studies of (Awu, *et al,* 2017) and (Abrahart *et al,* 2005).

Table 2: R and R^2 values for the ANN Model

Data Set	R-Value	R^2 Value
Testing	0.94385	0.89085
Training	0.9119	0.83156
Validation	0.93237	0.86931

Table 3: Water quality parameters error indices for ANN model

S/N	Water Quality Parameter	RMSE
1.	Electrical Conductivity	11.2
2.	Total Dissolved Solids	13.8
3.	Total Hardness	5.54

3.3 Multilinear Regression (MLR) Analysis

The MLR model was used as the standard approach to simulate the system's linear interactions. It frequently serves as the non-linear models' benchmark comparison model. In the ANN model calibration, a computer program of multiple regressions is used to obtain a set of coefficients for a linear model and determine how well the linear model represents the observed data (Muhammad *et al,* 2020).

Multiple linear regression (MLR) was applied in this work to justify the relationship between the water quality parameters. An MLR model takes the form:

$$Y = \beta_0 + \beta_1 x_1 + \beta_2 x_2 + \cdots + \beta_{p-1} x_{p-1} + \varepsilon$$

Where Y is the response variable, and there is p −1 explanatory variable, with p parameters (regression coefficients) $\beta_0, \beta_1, \beta_2 \ldots, \beta_{p-1}$,

This section deals with the development and results of electrical conductivity, total dissolved solids, and total hardness prediction models using MLR techniques using the best input combination based on the MATLAB (2016a) environment. The input parameters include pH and turbidity. The following regression models were derived, and the regression model equations are shown explicitly in Equations 3–5. The models are for the prediction of electrical conductivity (EC), total dissolved solids (TDS), and total hardness (TH).

$$Q_{(EC)} = \beta_0 + \beta_1 x_1 + \beta_2 x_2 + 11.2 \quad (3)$$

$$Q_{(TDS)} = \beta_0 + \beta_1 x_1 + \beta_2 x_2 + 13.8 \quad (4)$$

$$Q_{(TH)} = \beta_0 + \beta_1 x_1 + \beta_2 x_2 + 5.54 \quad (5)$$

Where x_1 and x_2 are input (independent) variables of pH and turbidity respectively. The other parameters are various estimated constants (β_0, β_1, β_2) generated by the ANN, as presented in Table 4 below. Thus, equations 6-8 above can be re-written as follows:

$$Q_{(EC)} = 84.266 + 0.38268x_1 - 0.19656x_2 \quad (6)$$

$$Q_{(TDS)} = 126.2 - 8.673x_1 - 0.13822x_2 \quad (7)$$

$$Q_{(TH)} = 41.98 - 1.1229x_1 + 0.047042x_2 \quad (8)$$

Table 4: Estimated constants for MLR model electrical conductivity, total dissolved solids and total hardness

	Estimate	SE	t-Stat	p-value	RMSE
β_0	73.066	25.54	2.8608	0.0055874	11.2
β_1	0.38268	3.6319	0.10537	0.91639	
β_2	-0.19656	0.15968	-1.231	0.22252	
β_0	112.41	31.368	3.5835	0.00062736	13.8
β_1	-8.673	4.4606	-1.9444	0.055926	
β_2	-0.13822	0.19611	-0.70478	0.48332	
β_0	36.44	12.605	2.8908	0.005133	5.54
β_1	-1.1229	1.7925	-0.62643	0.5331	
β_2	0.047042	0.078809	0.59691	0.55252	

3.4 Model Validation

To compare the goodness of fit of the ANN model, some representative hypothesis tests were conducted for the model construction process. These tests are the t-test to test the means and the F-test for variance. A paired t-test is used to compare the means of two sample populations, in which observations in one sample can be paired with observations in the other sample. The F-test is used to test if the variances of two populations are equal (Snedecor and Cochran, 1989), to further ascertain the performance efficiency of the predictive regression models, the R^2 and RMSE values for each were generated using Microsoft Excel.

3.4.1 F-Statistical Test

The F-test with two samples for variance was used to compare both the measured and predicted results. If F > Fcrit, the null hypothesis is rejected. Otherwise, it is accepted. Table 5 and 6 presents the results of the three analyses: For electrical conductivity, total dissolved solids, and total hardness as shown in Table 5, F is equal to 1.017605 and F critical is equal to 2.81793, suggesting that F crit is greater than F. Thus, the null hypothesis was accepted.

F value for total dissolved solids, as shown in Table 5, is equal to 1.670802 and Fcritical is equal to 2.81793, which clearly indicates that Fcritical is greater than F. Similarly, for total hardness, as shown in Table 5, F is equal to 2.307812 and Fcritical is equal to 2.81793, which shows that Fcritical is greater than F.

As a consequence, the null hypothesis is not rejected in any case since Fcritical is greater than F in all three analyses above. This means, however, that there is no significant difference between the measured and predicted model outcomes. Thus, the ANN model is valid and can be effectively used for the prediction of water quality parameters.

Table 5: F-Test two-sample for variances for electrical conductivity (Q_{EC}), total dissolved solids

	Measured	Predicted
Mean	77.53833	78.30528
Variance	32.64358	32.07883
Observations	12	12
Df	11	11
F	1.017605	
P(F<=f) one-tail	0.488715	
F Critical one-tail	2.81793	
Mean	46.2275	48.80959
Variance	7.379566	4.416782
Observations	12	12
Df	11	11
F	1.670802	
P(F<=f) one-tail	0.203914	
F Critical one-tail	2.81793	
Mean	27.02	29.84466
Variance	9.195982	3.984718
Observations	12	12
Df	11	11
F	2.307812	
P(F<=f) one-tail	0.090585	
F Critical one-tail	2.81793	

3.4.2 t-Test

When a t-test is performed, the null hypothesis is rejected if t stat > t critical two tails. Otherwise, it is accepted. Here, the paired-two sample for means was used. The results of the t-tests for electrical conductivity, total dissolved solids, and total hardness are shown in Table 6.

The result for electrical conductivity, as shown in Table 7, indicates that the value of the critical two tails is 2.200985 and the t start is -0.94542. The one for TDS, as shown in Table 5, indicates that t critical two tails has a value of 2.200985 and t stat has a value of -2.42495. Also, the total hardness as shown in Table 6 indicates that t critical two tails has a value of 2.200985 and t stat has a value of -5.15467. The outcomes of all three analyses, as clearly seen in the respective tables, show that t critical is greater than t stat. Thus, the null hypothesis is accepted. Hence, the model can be effectively used to predict the water quality parameters stated above.

Table 6: t-Test: Paired two sample for means for electrical conductivity (Q_{EC}) total dissolved solids

	Measured	Predicted
Mean	77.53833	78.30528
Variance	32.64358	32.07883
Observations	12	12
Pearson Correlation	0.87802	
Hypothesized Mean Difference	0	
Df	11	
t Stat	-0.94542	
P(T<=t) one-tail	0.182374	
t Critical one-tail	1.795885	
P(T<=t) two-tail	0.364749	
t Critical two-tail	2.200985	
Mean	46.2275	48.80959
Variance	7.379566	4.416782
Observations	12	12
Pearson Correlation	-0.15846	
Hypothesized Mean Difference	0	
Df	11	
t Stat	-2.42495	
P(T<=t) one-tail	0.016855	
t Critical one-tail	1/795885	
P(T<=t) two-tail	0.03371	
t Critical two-tail	2.200985	
Mean	27.02	20.84466
Variance	3.984713	3.984718
Observations	12	12
Pearson Correlation	0.791071	
Hypothesized Mean Difference	0	
Df	11	
t Stat	5.15467	
P(T<=t) one-tail	0.000158	
t Critical one-tail	1.795885	
P(T<=t) two-tail	0.000316	
t Critical two-tail	2.200985	

3.4.3 RMSE and R^2 Values

The RMSE and R^2 values for each of the linear regression models as shown in Table 7 indicate that electrical conductivity, total dissolved solids, and total hardness have RMSE values of 5.36, 6.94, and 0.08, respectively. This clearly implies that the total hardness model has the lowest value and thus has the best predictive performance. Consequently, the R^2 values for electrical conductivity, total dissolved solids, and total hardness are 0.9925, 0.9462, and 0.8876, respectively, for the model output parameters. In each case, the R^2 was very close to 1, thereby indicating excellent predictive performance.

Table 7: RMSE and R^2 values of the MLR models

Model	RMSE	R^2
Electrical Conductivity	5.36	0.9925
Total Dissolved Solids	6.94	0.9462
Total Hardness	0.08	0.8876

3.5 Water Quality Parameters Prediction (Forecast)

The predictions for electrical conductivity, total dissolved solids, and total hardness for a period of 2023–2029 are presented in figures 6–8. The model, which is a general representation of a system, is implored in the study for explanation of the water quality parameters being modelled, while the forecast model was used to predict future outcomes based on the current data. The R^2 values for the forecast are 0.999, 0.9487, and 0.9998 for electrical conductivity, total dissolved solids, and total hardness, respectively. All the R^2 values are very close to 1, indicating 99.9%, 94.8%, and 99.9% of the variance in the dependent variable is predictable from the independent variable. Thus, the forecasts and predictions for all three models are very effective and reliable.

4.0 CONCLUSION

Results obtained indicate that pH, which has a range of 6.45–8.5, and turbidity, which has a range of 1.6–36.21 NTU, were above the NSDWQ standard. TDS, EC, and total hardness, which have a range of 6.5–110.7 mg/l, 16.8–89.9 µS/cm, and 21.5–63.0 mg/l, respectively, were within the NSDWQ permissible standard. The performance of ANN was tested using RMSE, R, and R^2. The R^2 values obtained from the water quality parameters (electrical conductivity, total dissolved solids, and total hardness) and prediction were very close to 1, indicating a good model and prediction. The R values for the ANN testing, training, and validation data sets are 0.94385, 0.9119, and 0.93237, respectively. Consequently, the corresponding R^2 values are 0.89085, 0.83156, and 0.86931. Furthermore, the ANN RMSE values for EC, TDS, and TH are 11.2, 13.8, and 5.54, respectively. Multilinear Regression Model equations were obtained for predicting electrical conductivity, total dissolved solids, and total hardness. The R^2 values obtained for EC, TDS, and TH are 0.9925, 0.9462, and 0.8876, respectively. The corresponding RMSE values are 5.36, 6.94, and 0.08. Each of the mathematical equations is very effective for prediction. The model validation carried out through the F-test and t-test for each of electrical conductivity, total dissolved solids, and total hardness, respectively, shows that F critical is greater than F, as well as t critical is greater than t-stat. This further shows that the ANN model is fit for prediction. ■

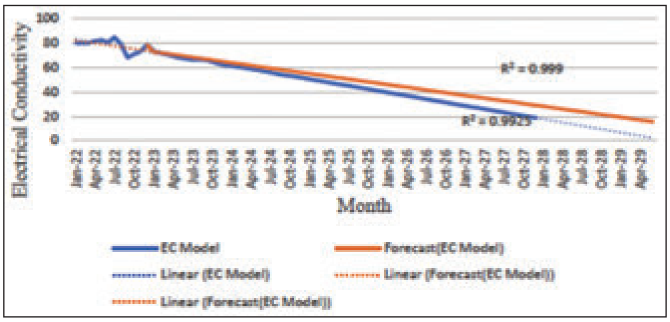

Figure 6: Prediction for EC model (2023-2029)

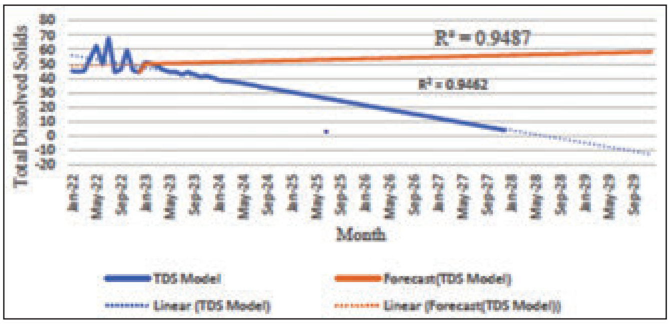

Figure 7: Prediction for TDS model (2023-2029)

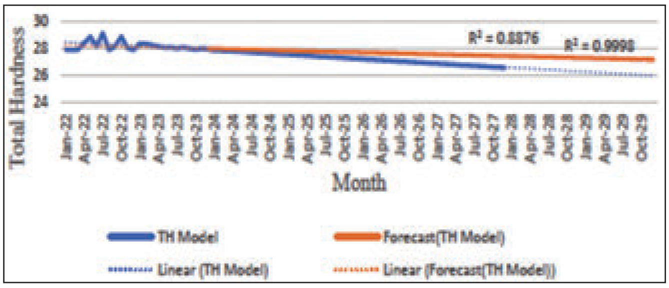

Figure 8: Prediction for total hardness model (2029-2029)

REFERENCES

[1] Ehya, F., & Saeedi, F. (2019). Assessment of groundwater quality in the Garmez area (Southeastern Khuzestan Province, SW Iran) for drinking and irrigation uses. Carbonates and Evaporites, 34(4), 1443-1454.

[2] Boretti, A., & Rosa, L. (2019). Reassessing the projections of the World Water Development Report. NPJ Clean Water, 2(15), 1-6.

[3] Egbueri, J. C., Mgbenu, C. N., & Chukwu, C. N. (2019). Investigating the hydrogeochemical processes and quality of water resources in Ojoto and environs using integrated classical methods. Modeling Earth Systems and Environment, 5(4), 1443-1461.

[4] Mrunmayee, M. S. (2014). Analysis and modelling of surface water quality in river basins (MTech Research Thesis, NIT Rourkela).

[5] Singh, K. P., Malik, A., & Sinha, S. (2005). Water quality assessment and apportionment of pollution sources of Gomti River (India) using multivariate statistical techniques: A case study. Analytica Chimica Acta, 538(1-2), 355-374.

[6] Marjan, S., Ehsan, T., & Zeinab, N. (2021). Application of an artificial neural networks model estimating of water quality parameters in Karun River Iran. Journal of Environmental Treatment Techniques, 9(4), 1710-1719. https://doi.org/10.4277/JETT/9(40)727

[7] Uba, J. I., Orakwe, L. C., Ogbu, K. N., Awu, J. I., Ahaneku, I. E., & Chukwuma, E. C. (2021). Forecasting water quality parameters using artificial neural network for irrigation purposes. Scientific Reports, 11, Article 24438. https://doi.org/10.1038/s41598-021-03435-6

[8] Elias, E., Sam, K., & Tahima, A. (2023). Aquaculture 4.0: Hybrid neural network multivariate water quality parameter forecasting model. Scientific Reports, 13, Article 16129. https://doi.org/10.1038/s41598-023-45678-y

[9] Jitha, P. N. (2023). Design and development of efficient water quality prediction models using variants of recurrent neural networks. NR Chem. Bull., 12(Special Issue 5), 1210-1223. https://doi.org/10.31838/ecb/2023.12.5.5.014

[10] Furaun, R., Abid, I., Sayyidi, T. K., Isabel, de la T. D., Juan, L. V. M., Carmen, L. R., & Imran, A. (2022). An artificial neural network for water quality and water consumption prediction. Water, 14(2), 3359. https://doi.org/10.33901/w/42133591

[11] Nguyen, T. H., Phan, D. T., & Dinh, T. N. (2018). Water quality evaluation of the Tien River by means of Water Quality Index (WQI) and statistical techniques. Vietnam Journal of Science and Technology, 56(2), 141-148.

[12] ASCE Task Committee. (2000). Artificial neural network in hydrology. I: Preliminary concepts. Journal of Hydrologic Engineering, 5(2), 115-123.

[13] Archana, S., & Prashant, P. (2015). River water quality modelling using artificial neural network technique. Aquatic Procedia, 4, 1070-1077.

[14] Ali, N., Ahmed, E., Othman, A. K., & Othman, J. (2009). Prediction of Johor River water quality parameters using artificial neural networks. European Journal of Scientific Research, 28(3), 422-435.

[15] Roza, D., & Mohsen, S. (2021). Artificial neural network system. International Journal of Imaging and Robotics, 21(2), 14-25.

[16] Khandelwal, M., & Singh, T. (2005). Prediction of mine water quality by physical parameters. Journal of Scientific and Industrial Research, 64(7), 564-570.

[17] Awu, J. I., Mbajiorgu, C. C., Ogunlela, A. O., Kasali, M. Y., Ademiluyi, Y. S., & James, D. D. (2017). Optimization of neural network architecture and transfer functions for rainfall river flow modeling. Journal of Environmental Hydrology, 25(8), 1-15.

[18] Abrahart, R. J., Kneale, P. E., & See, L. M. (2005). Neural networks for hydrological modelling. In R. J. Abrahart, P. E. Kneale, and L. M. See (Eds.), Hydroinformatics in hydrology, hydrogeology and water resources (pp. 223-250). Taylor and Francis Group.

[19] Muhammad, S. G., Sani, I. A., Aliyu, M. A., Abubakar, I. T., Mubarak, A. S., Parvaneh, E., & Norhaliza, A. (2020). Estimation of water quality index using artificial intelligence approaches and multi-linear regression. IAES International Journal of Artificial Intelligence (IJ-AI), 9(1), 126-134.

[20] Snedecor, G. W., and Cochran, W. G. (1989). Statistical methods (8th ed.). Iowa State University Press.

PROFILES

HARUNA GARBA is a senior lecturer in the Department of Civil Engineering, Nigerian Defence Academy (NDA) Kaduna, an Engineer with The Council for Regulation of Engineering in Nigeria and a member of Nigerian Society of Engineers. Area of specialisation is Hydrology and River Flow Dynamics. Area of research interest include Surface and Ground Water Hydrology and Climate Change.
Email address: hgarba@nda.edu.ng

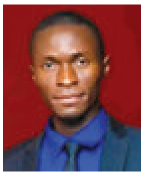

FRANCIS PETER is a distinct and dynamic individual with a great passion for research, academic excellence, and knowledge impartation, aiming to build a robust career in the engineering profession and beyond. He is currently the Vice Principal Administration of Standard Foundation Schools, Barnawa, as well as a chief consultant in health, safety, and environmental management with Zeteo Citadel, Kaduna State, Nigeria.
Email address: edokapeter2014@gmail.com

THE EFFECT OF DIFFERENT CUTTING TOOL MATERIALS AND MACHINING PARAMETERS ON THE SURFACE ROUGHNESS OF BIOMEDICAL-GRADE TITANIUM ALLOYS

Yathava Arulappan[1*], Yuvan Mailvahanam[2], A N M Tahmid Hossain Bhuyan[3]

Abstract

Titanium alloy (Ti6Al4V) is one of the hardest and strongest alloys used in modern manufacturing industries, particularly in medical implants, due to its exceptional strength-to-weight ratio, high corrosion resistance, and lightweight properties. This study investigates the impact of different cutting tool materials and machining parameters on the surface roughness of biomedical-grade titanium alloy. The research is motivated by the alloy's low thermal conductivity and strong chemical affinity with cutting tool surfaces at high temperatures, which complicates machining. The Taguchi method was employed to optimise machining parameters. Results show that cutting speed and depth of cut significantly influence the surface roughness of the titanium alloy. Using a tungsten carbide insert, the surface roughness achieved was 0.957 µm with machining parameters set at 125 m/min, 0.05 mm/rev, and 1.5 mm. In contrast, employing a polycrystalline diamond insert yielded the lowest surface roughness of 0.316 µm at the minimum cutting speed and depth of cut, with parameters of 68 m/min, 0.1 mm/rev, and 1.0 mm. This improvement is attributed to the low friction coefficient and excellent heat conductivity of polycrystalline diamond. However, the study has limitations in optimising other crucial machining performance factors, such as tool wear, cutting forces, and temperature generation. Further investigation into the combined effects of these parameters on the machining process is necessary to achieve optimal outcomes.

Received: *7 June, 2024*
Revised: *13 July, 2024*
Accepted: *7 August, 2024*

[1,3]Faculty of Mechanical Engineering, Universiti Teknologi Malaysia, 81310 Skudai, Johor, Malaysia.

[2]Faculty of Mechanical Engineering & Technology, Universiti Malaysia Perlis, 02600 Arau, Perlis, Malaysia.

****Corresponding author:***
yathava9479@gmail.com

Keywords:
Depth of cut, Polycrystalline diamond insert, Surface roughness, Titanium alloy,Tungsten carbide insert

1.0 INTRODUCTION

Titanium alloy (Ti-6AL-4V) is one of the most utilised alloys across various industries, particularly in medical applications. This alloy is notable for its hardness, surpassing certain steel grades while remaining lightweight. Its applicability in medical instruments derives from its durability, low weight, and exceptional corrosion resistance (Moran *et al.,* 2022). Ti-6AL-4V is extensively employed in the biomedical sector for producing orthopedic, cardiovascular, and dental implants due to its low thermal conductivity, high yield strength (reaching 550-600 °C), and excellent biocompatibility (Hwang *et al.,* 2020; Festas *et al.,* 2020).

Machining Ti6AL-4V presents significant challenges primarily due to its high hardness, ductility, and formidable strength. The processing of titanium-based biocompatible materials for implants is complex, especially when producing intricate geometrical features with surface quality (Salikhyanov *et al.,* 2022; Dagara *et al.,* 2018). The critical factor for medical implants is the surface roughness of machined biomedical-grade alloy, which plays a key role in determining their quality. Manufacturers enhance their operations by examining how machining parameters and cutting inserts affect surface roughness. The material's low thermal conductivity can lead to significant temperature increase due to strong interaction between the cutting tool and workpiece, resulting in a reduced tool lifespan. Its machinability is further compromised by low elastic modulus and high strength, which persist at elevated temperatures (Khalik *et al.,* 2023; Palanikumar *et al.,* 2022).

Additionally, cutting temperatures can escalate to exceptionally high levels, leading to chatter and fluctuations during machining. An increased tool wear rate directly deteriorates the quality of the machined surface. Throughout the machining process, it is crucial to meet various conditions, such as minimising time spent and maintaining a low cost per unit of material. Furthermore, excessive trial runs should be avoided. Identifying the optimal combination of cutting variables that satisfy all output criteria can be challenging under these constraints (Ma *et al.,* 2024; Khan & Maity, 2018).

Numerous studies have been conducted to discover effective methods for enhancing the machinability of titanium alloys. High-speed steel (HSS) cutting tools are one type of tool used for machining titanium alloys. It convincingly demonstrates that HSS tools become ineffective for machining titanium and similar alloys when the cutting speed is too high, for example greater than 30 meters per minute (Rahman *et al.,* 2006). Consequently, it is possible to process both highly alloyed and general-purpose grades of titanium. However, it is always a significant concern that the cutting speed should not be over the limit, which is 30 meters per minute.

Alternatively, tungsten carbide inserts can be utilised for machining titanium alloys. Their higher resistance to abrasive wear compared to HSS tools ensures longer tool life and consistent performance under high-stress conditions, where less durable materials may wear out rapidly. Nevertheless, tungsten carbide inserts have their limitations. Despite their exceptional performance under normal circumstances, they are susceptible to thermal shock during intermittent cutting of titanium alloys. This potentially leads to cracking and premature tool failure. Although tungsten carbide withstands higher temperatures compared to HSS, it possesses lower thermal conductivity, leading to increased cutting-edge temperatures that affect tool life and workpiece integrity (Masek *et al.,* 2022; Noor & Musfirah, 2022).

Another machining method for titanium alloys employs Polycrystalline Diamond (PCD) inserts. Research by F. Nabhani in 2001 demonstrated that PCD tools significantly reduce tool wear during titanium machining. As titanium carbide forms a protective coating on the tool's rake during machining, PCD tools remain effective even under challenging conditions. According to Chauhan *et al.* (2023), diamond is the most durable cutting tool material in the machining industry, with PCD specifically demonstrating a low friction coefficient that enhances wear resistance compared to other materials. PCD inserts attain high surface polish while significantly extending tool life and minimising the frequency of tool changes and interruptions, which is particularly advantageous for prolonged cutting processes (Sadik *et al.,* 2019).

The relationship between surface roughness of titanium alloys and various cutting tool materials and turning parameters has been the subject of several studies. A study by J. Nithyanandam *et al.* (2015) characterised surface roughness when turning titanium alloy with nanocoated carbide inserts, focusing on parameters such as cutting speed, nose radius, feed, and depth of cut. Their findings indicated that the feed rate had the most significant impact on surface roughness, followed by cutting speed, nose radius, and depth of cut.

Meanwhile, Abdelnasser *et al.* (2020) conducted research on conventional machining of biomedical-grade Titanium alloy using a PCD insert. The dry machine was utilised with a length of cut of 30mm and a diameter of 25mm. The results showed that showed that higher cutting speeds reduced surface roughness, primarily due to work material softening and decreased cutting force. However, increases in cutting speed also led to increased surface roughness caused by a phenomenon known as "chatter."

In a separate study by Yilmaz *et al.* (2020), the workpiece material was 7075 aluminium alloy (AA7075) with carbide cutting tools. Three feed rate values (0.05, 0.15, and 0.25 mm/rev), and three cutting speeds (190, 280, and 375 m/min) were tested while maintaining a constant cutting depth of 0.5 mm. The research revealed that rise in the feed rate significantly affected surface roughness, while an increase in cutting speed had minimal impact.

Therefore, most prior research has concentrated on a single cutting tool insert approach to assess the influence of surface roughness on titanium alloy. There is a critical need for further investigation as existing literature lacks a comprehensive analysis of how different cutting tool materials and machining parameters impact the surface roughness of the alloy. This study aims to explore two distinct cutting tool inserts while assessing various machining parameters including feed rate, cutting speed, and cutting depth to investigate their influence on achieving high-quality surface finishes for titanium alloys intended for biomedical implant applications. The primary objective is to identify the most influential machining parameter and evaluate the surface roughness of titanium alloy, subsequently examining how different turning parameters affect the surface roughness of biomedical-grade titanium alloy through the usage of both tungsten carbide and PCD inserts.

2.0 EXPERIMENTAL SETUP AND PROCEDURE

2.1 Workpiece Material for the Research

The cylindrical workpiece material chosen for this research was Biomedical-grade Titanium alloy (Ti-6Al-4V) with the length of 100mm and diameter of 25 mm. The Ti-6Al-4V's mechanical properties and chemical composition that are used in this experiment, are presented in Tables 1 and 2 as per the American Iron and Steel Institute standard (AISI).

Table 1: Titanium Alloy's (Ti-6Al-4V) physical properties

Mechanical Properties	Values
Ultimate Tensile Strength (MPa)	1170
Tensile Strength, Yield (MPa)	1100
Modulus of Elasticity (GPa)	114
Shear Modulus (GPa)	44
Elongation at break (%)	10
Poisson's Ratio	0.342

Table 2: Titanium Alloy's (Ti-6Al-4V) chemical composition

Elements	Content (%)
Titanium (Ti)	90
Aluminium (Al)	6
Vanadium (V)	4
Iron (Fe)	0.25
Oxygen (O)	0.2

2.2 Cutting Tool

A PCD insert, and Tungsten carbide insert were used in this project. The turning operation is conducted by using a conventional lathe machine. The machine used for this project is the Pinacho SP/165 Conventional lathe machine. The speed of cutting is expressed from m/min to revolutions per minute (RPM) to align with conventional lathe programming commands. Meanwhile, Band Saw Horizontal, HB 280 B machine is used to cut the Titanium alloy into required pieces for the experiment.

2.3 Experiment Set Up

The Band Saw Horizontal, HB 280 B machine was used to cut a 1000mm rod of biomedical-grade Titanium alloy into nine pieces, each 100 mm in length. After cutting, nine pieces are prepared for the experiment. The experiment involved cutting a length of 30 mm from each end of the rod using an external turning operation. One end of the rod was cut by using a Tungsten Carbide insert while the other end of the rod was cut by using a PCD insert. The cutting speeds used on a lathe machine were 68, 110, and 125 m/min, combined with feed rates of 0.05, 0.1, and 0.15 mm/rev, and cutting depths of 0.5, 1.0, and 1.5mm. A total of 18 experiments were conducted using the Taguchi method on both ends of the titanium alloy. Each titanium alloy rod was labelled with plastic tape for easy identification during the analysis phase to measure surface roughness.

Next, the Mitutoyo Surface Roughness Measuring Tester, model SJ-410 (SURFTEST SJ-410), was utilised to measure the surface roughness of the alloy. Before the measurement, the surface of the samples was cleaned and free of debris to make sure the data obtained was precise. Then, a Vee-block was used to support the Titanium alloy sample to free it from any unnecessary movement while taking the measurement. The standard parameter for surface roughness in this experiment was the average surface roughness, Ra. The tester was positioned on the titanium alloy's surface to conduct the measurement, with the device probe traversing the surface for 20 mm and recording the height variations that comprise the surface texture. After measurement, the device displayed the results, which were recorded for further analysis. The average surface roughness measurements (Ra) were plotted on the y-axis, while different machining parameters—such as cutting speed (m/min), feed rate (mm/rev), and depth of cut (mm)—were plotted on the x-axis for both inserts to study their influence on surface roughness.

Additionally, an Optical Microscope, model XST60 was used to observe the surface of sample that has the highest and lowest surface roughness obtained for both inserts. First, the interpupillary distance was adjusted by moving the eyepieces closer or further apart until a single circular field was visible. Then, the selected four samples were placed on the specimen slide one by one and secured with the Vee-block. The lens magnification used to examine the sample surfaces was 20x. For optimal clarity, the diaphragm was adjusted to control the light on the titanium alloy samples. Finally, the images obtained from the microscope were saved in PDF format.

2.4 Taguchi Method

The Taguchi method was employed in the experiment to identify the optimal machining performance characteristics of the titanium alloy (Ti-6Al-4V). This approach ensures consistent results throughout the turning experiment. Table 3 shows that there are three acceptable factors, each with three levels. A crucial aspect of a parametric analysis is the selection of controlled parameters. The primary parameters considered for the experiment include cutting speed, feed rate, and depth of cut.

Table 3: The considered parameters and levels for the experiment

Factor	Cutting Parameters	Level			Unit
		1	2	3	
1	Cutting speed	68	110	125	m/min
2	Feed rate	0.05	0.1	0.15	mm/rev
3	Depth of Cut	0.5	1.0	1.5	mm

Additionally, the orthogonal array L9 is used to execute the experiment. As a result, Table 4 displays the orthogonal array type L9 with a variety of parameters.

Table 4: Table of Taguchi design for the experiment (Orthogonal Arrays L9)

Experiment Number	Cutting Parameter Level		
	A	B	C
	Cutting Speed	Feed Rate	Depth of Cut
1	1	1	1
2	1	2	2
3	1	3	3
4	2	1	2
5	2	2	3
6	2	3	1
7	3	1	3
8	3	2	1
9	3	3	2

The parameter selection in Table 5 using the Taguchi technique was conducted in the machining process to identify the impact of cutting tool materials with machining parameters on performance of machining for the workpiece. A total of 18 experiments were conducted on both end sides of the workpiece using the presented cutting parameter level in Table 5.

Table 5: The layout of the experiment is based on an L9 orthogonal array for the research

Number of Experiment	Cutting Parameter Level			Diameter (mm)
	A	B	C	
PCD Insert	Cutting Speed (m/min)	Feed Rate (mm/rev)	Depth of Cut (mm)	
	68	0.05	0.5	25
	68	0.1	1.0	25
	68	0.15	1.5	25
	110	0.05	1.0	25
	110	0.1	1.5	25
	110	0.15	0.5	25
	125	0.05	1.5	25
	125	0.1	0.5	25
	125	0.15	1.0	25
Tungsten carbide insert				
	68	0.05	0.5	25
	68	0.1	1.0	25
	68	0.15	1.5	25
	110	0.05	1.0	25
	110	0.1	1.5	25
	110	0.15	0.5	25
	125	0.05	1.5	25
	125	0.1	0.5	25
	125	0.15	1.0	25

3.0 RESULTS AND DISCUSSION

3.1 Results

3.2 The Impact of Machining Parameters on the Surface Roughness of Biomedical-Grade Titanium Alloy Utilising a Tungsten Carbide Insert

The surface roughness of biomedical-grade titanium alloy is significantly influenced by machining parameters, which vary based on the cutting inserts used. When employing a tungsten carbide insert, higher cutting speeds and depths of cut result in a notable increase in surface roughness. The lowest recorded surface roughness is 0.366 μm, while the maximum is 0.954 μm, achieved during experiments 1 and 7, respectively. It was observed that increasing the depth of cut strongly affects the surface roughness of the titanium alloy, leading to visible deterioration in surface quality.

In addition to machining parameters, it is noteworthy that tungsten carbide inserts have weaker wear properties compared to PCD inserts. PCD inserts provide superior wear resistance, even at high cutting speeds. During the machining of titanium alloy, generated heat is effectively dissipated from the cutting area, helping to prevent thermal workpiece deformation, and minimising heat-induced surface irregularities.

Figure 1 shows the relationship between surface roughness against the influence of feed rate on cutting speed using tungsten carbide method. As the feed rate increases, surface roughness gradually rises. Initially, there is a linear increase in surface roughness for feed rates of 0.05 mm/rev and 0.10 mm/rev with cutting speeds ranging from 68 m/min to 110 m/min. However, at feed rates of 0.05 mm/rev and 0.15 mm/rev, a significant change in surface roughness occurs when cutting speeds increase from 110 m/min to 125 m/min. This is due to the crucial role of depth of cut in determining surface roughness at these feed rates. Specifically, a depth of cut of 1.5 mm at a feed rate of 0.05 mm/rev increases the tool and workpiece contact area, exerting more strain on the tungsten carbide insert.

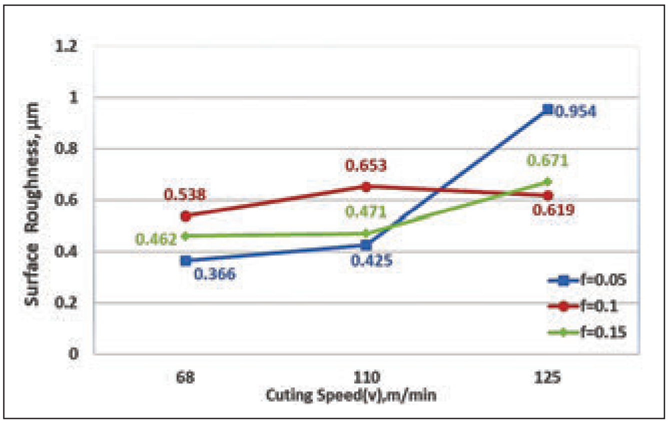

Figure 1: Graph of surface roughness against the influence of feed rate on cutting speed using Tungsten Carbide inserts

Table 6: Result of average surface roughness during machining process on Polycrystalline diamond and Tungsten carbide inserts

Number of Experiment	Cutting Parameter Level			Diameter (mm)	Spindle Speed (RPM)	Average Surface Roughness (μm)
	A	B	C			
Polycrystalline Diamond insert (PCD)	Cutting Speed (m/min)	Feed Rate (mm/rev)	Depth of Cut (mm)			
1	68	0.05	0.5	25	860	0.347
2	68	0.1	1.0	25	860	0.310
3	68	0.15	1.5	25	860	0.615
4	110	0.05	1.0	25	1400	0.424
5	110	0.1	1.5	25	1400	0.425
6	110	0.15	0.5	25	1400	0.531
7	125	0.05	1.5	25	2000	0.429
8	125	0.1	0.5	25	2000	0.516
9	125	0.15	1.0	25	2000	0.582
Tungsten carbide insert						
1	68	0.05	0.5	25	860	0.366
2	68	0.1	1.0	25	860	0.538
3	68	0.15	1.5	25	860	0.462
4	110	0.05	1.0	25	1400	0.524
5	110	0.1	1.5	25	1400	0.653
6	110	0.15	0.5	25	1400	0.471
7	125	0.05	1.5	25	2000	0.954
8	125	0.1	0.5	25	2000	0.619
9	125	0.15	1.0	25	2000	0.671

Conversely, a feed rate of 0.15 mm/rev with a depth of cut of 1 mm results in less heat generation, leading to less impact on surface roughness compared to a feed rate of 0.05 mm/rev. Consequently, the tool's cutting edge distorts and wears down, resulting in a rougher workpiece surface during the turning operation. Further evidence of this is seen in the fluctuation of surface roughness values at a feed rate of 0.10 m/rev, where an initial increase is followed by a slight decrease. The significant role of depth of cut in determining the surface roughness of titanium alloy is underscored by the observed variations. These variations arise from differences in depth of cut values, with a setting of 1.5 mm at a cutting speed of 110 m/min compared to 0.5 mm at a cutting speed of 125 m/min.

Figure 2 illustrates the relationship between surface roughness against the influence of cutting speed on depth of cut using Tungsten Carbide inserts. The graph shows that surface roughness initially increases as the depth of cut rises across all cutting speed levels, except at a cutting speed of 68 m/min. At 68 m/min, surface roughness increased from 0.366 μm to 0.538 μm but then decreased back to 0.462 μm. This phenomenon is attributed to the relatively low cutting speed, which results in less heat generation, thus having a minimal effect on the surface roughness of titanium alloy. Given that titanium alloy has low thermal conductivity, this property has been safe from this heat generation.

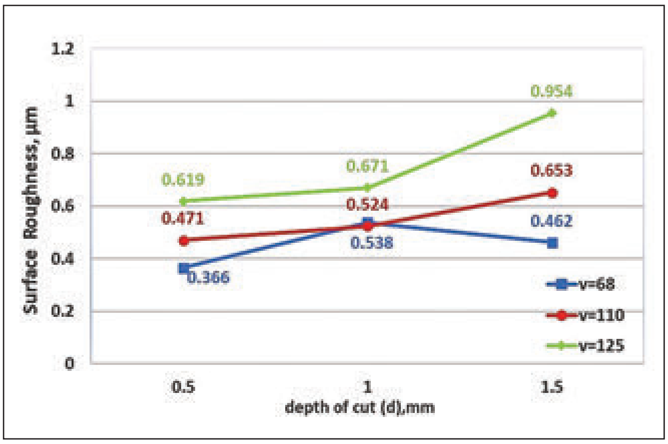

Figure 2: Graph of surface roughness against the influence of cutting speed on depth of cut using Tungsten Carbide inserts

Furthermore, a correlation exists where an increase in cutting depth leads to higher surface roughness across various cutting speeds, although the rate of increase varies. For example, at a cutting speed of 110 m/min, the difference in surface roughness between a 1 mm and a 1.5 mm increases to 0.283 μm. This comparison underscores the varying impact of cutting depth on surface roughness at different cutting speeds. Clearly, increased cutting speeds combined with greater cutting depths lead to elevated temperatures when machining titanium alloys with tungsten carbide inserts. The rise in temperature results from increased friction between the cutting tool and the workpiece at higher speeds and depths, leading to greater heat generation. Consequently, this thermal effect facilitates the formation of burrs and built-up edges (BUE) on the workpiece surface under such high-temperature conditions.

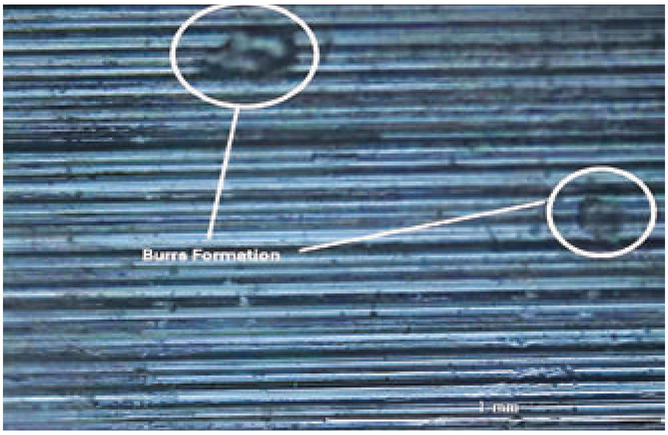

Figure 3: Diagram of Titanium alloy with highest surface roughness using Tungsten Carbide insert

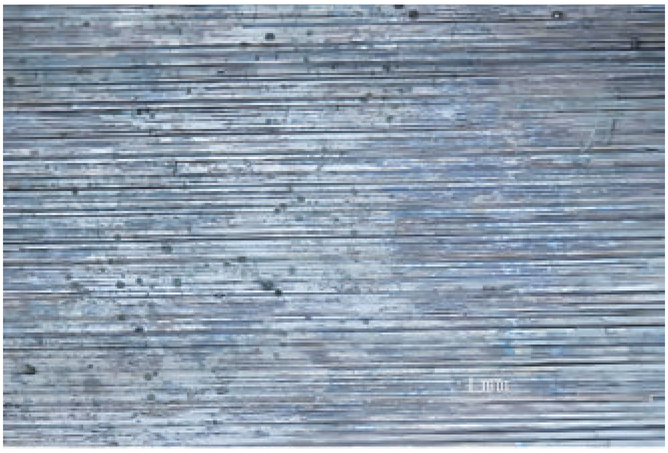

Figure 4: Diagram of Titanium alloy with lowest surface roughness using Tungsten Carbide insert

As evident, figures 3 and 4 show the diagram of Titanium alloy surface with the highest surface roughness and lowest surface roughness using the Tungsten Carbide insert which was observed through optical microscope at a magnification of 20x, respectively.

The highest surface roughness value obtained was 0.954 μm with the parameter setting of 125m/min, 0.05mm/rev and 1.5mm. It's obvious to see that the Titanium alloy surface has developed some burrs, an imperfection in the shape of deformed material that sticks out from the surface. It is usually linked to aggressive machining conditions or poor cutting parameters that fail to control the material flow.

There are no apparent imperfections or burrs in the surface, suggesting a smoother and more regular surface texture. The lowest surface roughness recorded was 0.366 μm with the machining parameter of 68m/min, 0.05mm/rev and 0. 5mm. This suggests that the machining parameters were fine-tuned for this sample, leading to a superior finish.

3.3 The Impact of Machining Parameters on the Surface Roughness of Biomedical-Grade Titanium Alloy Utilising Polycrystalline Diamond Insert

The utilisation of PCD inserts resulted in achieving a minimum surface roughness of 0.310 μm, while the maximum surface roughness of 0.615 μm was attained during experiments 2 and 3.

Figure 5 shows the relationship between surface roughness against the influence of feed rate on cutting speed using PCD insert. Initially, surface roughness increases for all feed rates except for the rate of 0.15 mm/rev as cutting speed varies from 68 m/min to 110 m/min. There is an approximate twofold increase in surface roughness, rising from 0.31 μm to 0.615 μm when the feed rate increases from 0.10 mm/rev to 0.15 mm/rev at a cutting speed of 68 m/min. The primary factor contributing to the spike in surface roughness is the cutting depth chosen for the experiment, where the feed rate of 0.15 mm/rev corresponds to a depth of 1.5 mm, higher than the other depths of cut, which are 0.5 mm and 1 mm. Consequently, cutting temperatures increased directly in proportion to the cutting depth, significantly affecting the final surface roughness of the titanium alloy.

The conducted research clearly indicates that surface roughness progressively increases with both rising feed rate and cutting speed when employing a PCD insert. In Experiment 1, the recorded surface roughness value was 0.347 μm at a feed rate of 0.05 mm/rev. This was succeeded by a higher surface roughness value of 0.425 μm in Experiment 5, where the feed rate was 0.10 mm/rev. Ultimately, during Experiment 9, using a feed rate of 0.15 mm/rev, the surface roughness value further increased to 0.582 μm. Utilising PCD tools for titanium machining notably reduces tool wear due to the formation of a protective titanium carbide coating on the tool's rake face during the machining process. This titanium carbide forms when titanium from the workpiece reacts with carbon from the cutting tool at elevated temperatures. The chemical reaction between titanium and carbon leads to titanium carbide formation, which then bonds with the surface of the cutting tool. Therefore, PCD maintains its sharp cutting edge at high temperatures without deteriorating and produces less surface roughness on titanium alloy compared to tungsten carbide.

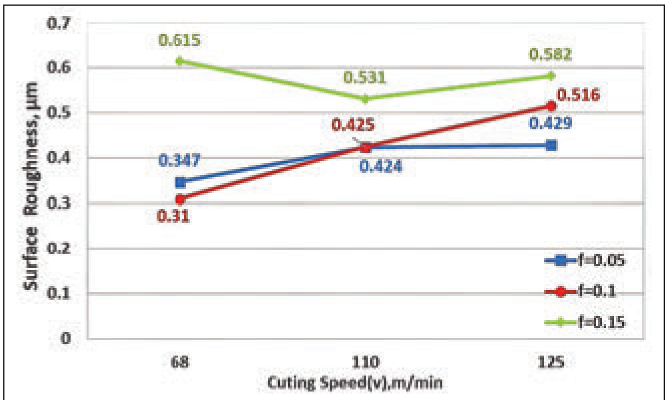

Figure 5: Graph of surface roughness against the influence of cutting speed on depth of cut using PCD insert

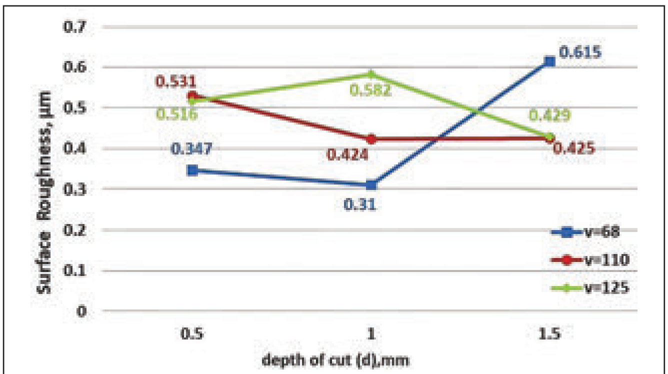

Figure 6: Graph of surface roughness against the influence of cutting speed on depth of cut using PCD insert

Figure 6 illustrates the relationship between surface roughness against the influence of cutting speed on depth of cut using PCD inserts. At a cutting speed of 68 m/min, the surface roughness initially decreases as the depth of cut increases from 0.5 mm to 1 mm, but then rises significantly when the depth of cut reaches 1.5 mm. In contrast, at a cutting speed of 110 m/min, surface roughness decreases from 0.5 mm to 1 mm, and remaining constant when the depth of cut increases to 1.5 mm. Lastly, at a cutting speed of 125 m/min, surface roughness increases from 0.5 mm to 1 mm, but decreases when the depth of cut reaches 1.5 mm.

The increase in surface roughness at lower depths of cut is primarily attributed to ploughing rather than chip formation. Additionally, surface roughness was slightly influenced by cutting speed at shallow depths. Specifically, at the slowest cutting speed of 68 m/min, a depth of cut of 0.5 mm resulted in the smoothest surface, measuring 0.347 μm. Conversely, at the highest cutting speed of 125 m/min, the roughest surface recorded was 0.516 μm. At a cutting speed of 68 m/min and a depth of cut of 1.5 mm, the roughest surface roughness observed on titanium alloy using a PCD insert was 0.615 μm, representing the highest surface roughness recorded in this experiment. It was determined that cutting speed and depth of cut significantly influence surface roughness more than feed rate, with depth of cut showing the strongest effect on overall surface roughness when using PCD inserts.

Figures 7 and 8 show the diagram of Titanium alloy surface with the highest surface roughness and lowest surface roughness using the PCD insert which was observed through optical microscope at a magnification of 20x, respectively.

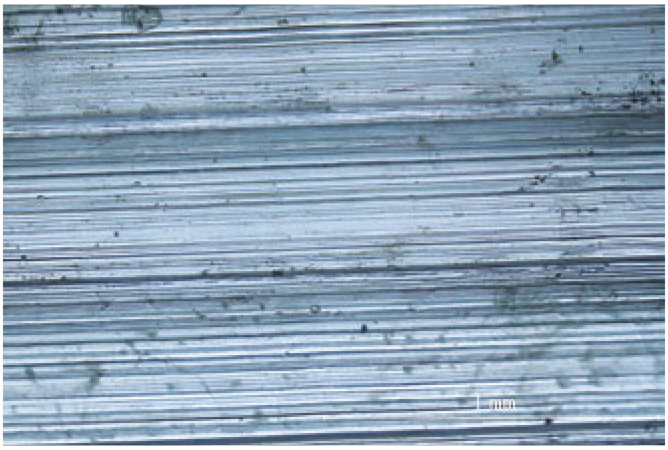

Figure 7: Diagram of Titanium alloy with highest surface roughness using PCD insert

The surface roughness value obtained was 0.615 μm which is the highest recorded using PCD insert using machining parameter of 68m/min, 0.15mm/rev and 1.5 mm. From the diagram, it clear that the finishing surface is much better as there is no significant burrs formations compared with Tungsten Carbide insert.

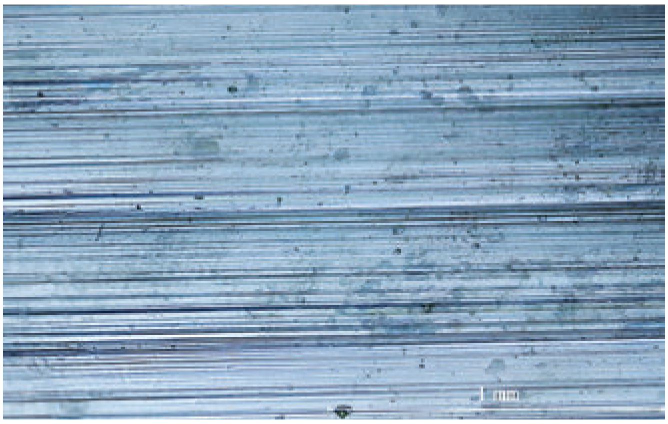

Figure 8: Diagram of Titanium alloy with lowest surface roughness using PCD insert

The lowest surface roughness value obtained was 0.310 μm which is overall the lowest surface roughness value with the parameter setting of 68m/min, 0.1mm/rev and 1.0mm obtained by using Tungsten Carbide insert. This clearly proves that PCD insert shows excellent performance in machining biomedical-grade titanium as it produces the best finishing surface. The Titanium alloy machined by using PCD insert could potentially be better suited for use as a medical implant.

4.0 CONCLUSION

The study successfully identified the surface roughness of biomedical-grade titanium alloy using PCD and tungsten carbide inserts. Based on the study's objectives, the results indicated that cutting speed and depth of cut have the most significant influence on surface roughness. Surface roughness increases significantly as cutting speed and depth increase. The maximum surface roughness achieved with a tungsten carbide insert was 0.954 μm, under machining parameters of 125 m/min, 0.05 mm/rev, and 1.5 mm. Conversely, the minimum surface roughness recorded with a PCD insert was 0.316 μm, corresponding to machining parameters of 68 m/min, 0.1 mm/rev, and 1.0 mm, representing the lowest cutting speed and depth of cut. This superior performance of the PCD insert is attributed to its low coefficient of friction and excellent heat conductivity, which contribute to finer surface finishes. The average surface roughness from nine experiments for each insert was calculated, showing an average of 0.584 µm for the tungsten carbide insert and 0.464 μm for the PCD insert. The slight deviations in average roughness values for both inserts stem from their good thermal conductivity, helping dissipate heat generated during machining.

Although both inserts yield similar average roughness, the PCD insert achieves a significantly better overall surface roughness due to its exceptional wear resistance, which allows it to withstand the abrasive wear typical of machining titanium alloys without significant tool wear. This durability keeps the cutting-edge sharp throughout the machining process, ensuring a consistent and smooth cutting action. However, the study has limitations in optimization, as it primarily focuses on surface roughness without thoroughly examining other crucial machining performance factors, such as tool wear, cutting forces, and temperature generation. Further investigation into the combined effects of these parameters on the machining process is necessary to achieve the best outcomes.

5.0 RECOMMENDATIONS FOR FUTURE WORK

A well-balanced combination of machining parameters including cutting speed, feed rate, and depth cut, along with the appropriate selection of cutting tool materials, plays a crucial role in the efficient machining of biomedical-grade titanium alloy. Several recommendations are proposed to enhance the reliability of the experiment:

1. **Use biocompatible coolants:** Traditional petroleum-based coolants can pose health risks. It is recommended to use water-soluble coolants or vegetable-based oils for medical implants. Exploring lubrication systems such as minimum quantity lubrication (MQL) or cryogenic cooling can significantly improve machining results. For instance, cryogenic cooling with liquid nitrogen can reduce thermal damage and enhance surface quality, thus increasing the biocompatibility of titanium implants.
2. **Compare cutting performance and tissue compatibility with other biomedical alloys:** For instance, cobalt-chromium and stainless steel. Cobalt-chromium is recognized for its wear resistance and is used in joint replacements, while stainless steel is cost-effective and easy to shape. By examining these attributes alongside those of titanium alloys, researchers can identify the optimal material for medical applications such as dental implants and bone fixation plates. This analysis will guide the development of more effective and biocompatible medical devices.
3. **Employ full factorial design:** Instead of the Taguchi method, which focuses on a subset of factors, a complete factorial design approach should be used to assess all potential combinations of factors and levels. For example, when examining the impact of cutting speed, feed rate, and type on the surface roughness of titanium implants, a full factorial design evaluates every possible combination of these variables. This method helps identify interactions among factors that might not be apparent in a partial analysis.
4. **Conduct ANOVA for improved accuracy:** Performing an Analysis of Variance (ANOVA) assesses the statistical significance of each variable and their interactions, ensuring that detected effects are not coincidental. Employing ANOVA to carefully consider the statistical significance of experimental results enhances the integrity and reliability of research conclusions.

6.0 ACKNOWLEDGEMENT

We gratefully acknowledge that all the workpieces for this research were provided by the Institution. No funding or grants were used for this research. We are immensely grateful to our co-authors, whose expertise, understanding, and patience was key in the completion of this work. ■

REFERENCES

[1] Chauhan, D., Makhesana, M. A., Rashid, R. a. R., Joshi, V., & Khanna, N. (2023). Comparison of Machining Performance of ti-6al-4v Under Dry and Cryogenic

Techniques Based on Tool Wear, Surface Roughness, and Power Consumption. Lubricants, 11(11), 493. https://doi.org/10.3390/lubricants11110493

[2] Dadgari, A., Huo, D., & Swailes, D. (2018). Investigation on Tool Wear and Tool Life Prediction in Micro-Milling of Ti-6Al-4V. Nanotechnology and Precision Engineering, 1(4), 218–225. https://doi.org/10.1016/j.npe.2018.12.005

[3] Festas, A., Ramos, A., & Davim, J. (2019). Medical Devices Biomaterials – A review. Proceedings of the Institution of Mechanical Engineers Part L. Journal of Materials Design and Applications, 234(1), 218–228. https://doi.org/10.1177/1464420719882458

[4] Hwang, Y., Choi, Y., Hwang, Y., Cho, H., & Lee, D. (2020). Biocompatibility and Biological Corrosion Resistance of TI–39NB–6ZR+0.45AL Implant Alloy. Journal of Functional Biomaterials, 12(1), 2. https://doi.org/10.3390/jfb12010002

[5] Khalik, M. A., Zahiri, S. H., Masood, S. H., Gulizia, S., Faizan-Ur-Rab, M., & Palanisamy, S. (2023). Simultaneous Densification and Improvement of Cold Spray Additively Manufactured Ti-6Al-4 V Properties via Electro-plastic Treatment. The International Journal of Advanced Manufacturing Technology, 126(9–10), 4297–4316.https://doi.org/10.1007/s00170-023-11401-5

[6] Khan, A., & Maity, K. (2018). Machinability Assessment of Commercially Pure Titanium (CP-Ti) During Turning Operation: Application Potential of GRA Method. IOP Conference Series Materials Science and Engineering, 338, 012005. https://doi.org/10.1088/1757-899x/338/1/012005

[7] Ma, H., Wang, J., Qin, P., Liu, Y., Chen, L., Wang, L., & Zhang, L. (2024). Advances in Additively Manufactured Titanium Alloys by Powder Bed Fusion and Directed Energy Deposition: Microstructure, Defects, and Mechanical Behavior. Journal of Material Science and Technology, 183, 32–62. https://doi.org/10.1016/j.jmst.2023.11.003

[8] Masek, P., Maly, J., Zeman, P., Heinrich, P., & Alagan, N. T. (2022). Turning of Titanium Alloy with PCD Tool and High-Pressure Cooling. Journal of Manufacturing Processes, 84, 871–885. https://doi.org/10.1016/j.jmapro.2022.10.034

[9] Moran, T. P., Carrion, P. E., Lee, S., Shamsaei, N., Phan, N., & Warner, D. H. (2022). Hot Isostatic Pressing for Fatigue Critical Additively Manufactured TI-6AL-4V. Materials, 15(6), 2051. https://doi.org/10.3390/ma15062051.

[10] Nabhani, F. (2001). Machining of Aerospace Titanium Alloys. Robotics and Computer-Integrated Manufacturing, 17(1–2), 99–106. https://doi.org/10.1016/s0736-5845(00)00042-9

[11] Noor, N. D., & Musfirah, A.H., (2022). Optimization of Cutting Parameter for Machining TI-6AL-4V Titanium Alloy. Journal of Modern Manufacturing Systems and Technology, 6(1), 53–57. https://doi.org/10.15282/jmmst.v6i1.7465.

[12] Palanikumar, K., Nithyanandam, J., Natarajan, E., Lim, W. H., & Tiang, S. S. (2023). Mitigated Cutting Force and Surface Roughness in Titanium Alloy-Multiple Effective Guided Chaotic Multi Objective Teaching Learning-Based Optimization. Alexandria Engineering Journal, 64, 877–905. https://doi.org/10.1016/j.aej.2022.09.029

[13] Rahman, M., Wang, Z., & Wong, Y. (2006). A Review on High-Speed Machining of Titanium Alloys. JSME International Journal Series C, 49(1), 11–20. https://doi.org/10.1299/jsmec.49.11

[14] Sadik, M. I., Coronel, E., & Lattemann, M. (2019). Influence of Characteristic Properties of PCD Grades on the Wear Development in Turning of β-titanium Alloy (Ti5Al5V5Mo3Cr). Wear, 426–427, 1594–1602. https://doi.org/10.1016/j.wear.2019.01.012

[15] Salikhyanov, D., Veselova, V., & Volkov, V. (2021). Flow Behavior and Microstructure Evolution of Ti-6Al-4V Titanium Alloy Produced by Selective Laser Melting Compared to Wrought. The International Journal of Advanced Manufacturing Technology, 119(1–2), 953–967. https://doi.org/10.1007/s00170-021-08000-7

LIST OF NOTATIONS

List of Abbreviations

AISI	American Iron and Steel Institute
BUE	Build-Up Edge
PCD	Polycrystalline Diamond
TC	Tungsten Carbide
Ti	Titanium

List of Symbols

MPa	Mega Pascal
Ra	Surface Roughness
%	Percentage
d	Depth of cut
f	Feed rate
v	Cutting speed
mm	Measurement for depth of cut
mm/rev	Measurement for feed rate
m/min	Measurement for Cutting speed
°C	Celsius

PROFILES

YATHAVA ARULAPPAN graduated with a degree in Mechanical-Aeronautical Engineering with honors from the University of Technology (UTM) in 2022. His studies mainly focus on Computational Fluid Dynamics (CFD) methods. These methods help him explore the unsteady aerodynamics of various objects like aircraft, helicopters, and wind turbines. Yathava is deeply involved in research concerning aircraft aerodynamics to make them more efficient. He aims to understand the complex unsteady flow structure better and experiment with advanced flow control techniques. Currently, his research interests include biomedical material, material science, flow control, and renewable energy.
Email address: yathava9479@gmail.com

YUVAN MAILVAHANAM graduated in 2023 with a Bachelor of Mechanical Engineering Technology with Honours from Universiti Malaysia Perlis (UniMAP). His expertise encompasses CNS Technology, noise and vibration, failure analysis, and sustainable engineering. Yuvan is dedicated to researching suitable machining techniques for sustainable engineering applications. His current research interests focus on improving machining processes to enhance their efficiency and sustainability in the engineering field. Passionate about innovation, Yuvan strives to bridge the gap between sustainable engineering and environmental responsibility.
Email address: ymailvahanam14@gmail.com

TAHMID HOSSAIN finished his Bachelor of Mechanical Engineering with honors at UTM in 2022. His focus was Biomechanics & Biomaterials, Computational Mechanics, and Failure Analysis. These subjects allow him to explore the inner workings of living tissues and cutting-edge materials. He dreams of upgrading biomedical materials for better medical equipment. Tahmid Hossain is passionate about researching energy storage systems and green energy solutions to enhance them. Currently, he is focused on Energy Storage Systems, Biomedical Materials, and Renewable Energy.
Email address: aabegtahmid@gmail.com

FUNDAMENTAL BASIC S-N CURVE TO STUDY FATIGUE LIFE OF R260 RAIL UNDER UNIAXIAL FATIGUE TESTING

M. N. Tawfik[1*], Mahfodzah Md Padzi[2], Shahrum Abdullah[3], Dani Harmanto[4]

Abstract

The main objective of this research paper is to examine the fatigue life of the R260 material specimen under uniaxial fatigue testing. Three specimens were selected to evaluate the value of ultimate tensile strength (UTS), ensuring a similar number using UTM, specifically below 250 kN. The specimens shape designed in requirement standard ASTM E8 for metal material. An experiment was conducted to determine fatigue life using eighteen bulk specimens in accordance with the standard ASTM E466-15 at seven different loading levels under uniaxial fatigue test. A Servo-Pulser fatigue machine was used with a performance of less than 100 kN, a sinusoidal signal frequency of 10Hz, and based on 20%, 30%, 35%, 40%, 45%, 55%, and 65% below the value of the ultimate tensile strength (UTS) of 1145 MPa. The value of stress ratio R= -1 was set up in the experiment as a principal to establish the S-N curve. The findings shows that the boundaries of low cycle fatigue regime occur at 65%, and high cycle fatigue regime occur at 35%, 40%, 45%, 55% and endurance limit occur at 20% & 30% for the total fatigue life cycles of R260. The study concludes that specific loading values significantly impact the fatigue life of the specimens, as observed from the trend in loading values. This approach is highly valuable and contributes to the known natural material behaviour related to fatigue life. This is not yet reported and it have not published yet in Malaysia light rail transit scenario.

Received: *13 June, 2024*
Revised: *8 August, 2024*
Accepted: *15 September, 2024*

[1,2]Mechanical Section, Malaysia France Institute, Universiti Kuala Lumpur, 43650, Kuala Lumpur, Malaysia.

[3]Department of Mechanical and Manufacturing Engineering, Universiti Kebangsaan Malaysia, 43600, Bangi, Malaysia.

[4]School of Mechanical and Aeronautical Engineering, De Montfort University, LE1 9BH, UK.

****Corresponding author:***
mahfodzah@unikl.edu.my

Keywords:
Fatigue life, Fatigue machine, R260 rail profile, S-N curve

1.0 INTRODUCTION

Light rail transit is one of the crucial methods of transportation used to support mobility for various purposes. It plays a pivotal role in assisting the domestic demand and accelerating the growth of the economy. In order to support daily railway operations, the problem of rolling contact fatigue has been identified and has appeared over many decades due to the different rail scenarios (Tawfik *et al.,* 2022; Kim *et al.,* 2014). The modern engineering community of railway infrastructure introduced the meaning of fatigue as the formation of a crack on two metal surfaces due to cyclic loading with various stresses, respectively (Tawfik *et al.,* 2022; Rui & Kaewunruen, 2022). The stress concentration and structural discontinuities are the main critical points on the surface linked to fatigue (Azmalea, 2024; Rui & Kaewunruen, 2022). It has the potential to propagate the crack becoming failure and damage (Pereira *et al.,* 2019; Dowling *et al.,* 2020). Gren *et al.* (2024) and Cini (2012) concur that a mechanical component forced under continuous loading either hundreds, thousands or millions of times can develop defects and cracks with an increasing likelihood of the failure of the component. The failure always appears gradually, locally, and permanently by relying on the repeated stress coming out of the dynamic stress in the critical area where the number of stresses it is subjected to are less than the ultimate tensile strength (Tawfik *et al.,* 2022; Shen; 2017).

In railway track systems, the R260 rail profile is one of the leading types of material used worldwide, including in the United Kingdom, Thailand and Malaysia (Padzi *et al.,* 2023; Tawfik *et al.,* 2023). It is original from steel and typically involves hot rolled steel, specifically in the manufacturing process (Azmalea, 2024). The main advantages of this material are good high strength, good elastic modulus, and good thermal resistance (Azmalea, 2024). It plays a crucial role in the budgeting of maintenance programs for return of investment and it is recognized through regulations by the government and performs well (Azmalea, 2024; Tawfik *et al.,* 2023). A research group from ASEAN countries found that mechanical parts require an examination for fatigue because they can experience catastrophic failure constraints over time and in loading service conditions (Mazlan *et al.,* 2020).

Rails are critical for assisting train movements and the direction of the route, as well as being involved in safety and reliability as part of rail transportation. Rails are mainly subjected to cycling loading which can generate the phenomena of fatigue in most stress areas under rail-wheel contact. Tawfik *et al.* (2022) defined rolling contact fatigue (RCF) as a term used to refer to rail track systems. The appearance of major failures due to the repeated stresses of rail-wheel contact happen when in dynamic mode. Numerous defects come from RCF including squad, shelling/spalling and head checking, which might be categorized as dangerous and are potential threat to the train due to the risk of derailment (Teng *et al.,* 2022). RCF happens in urban railways as shown in Figure 1.

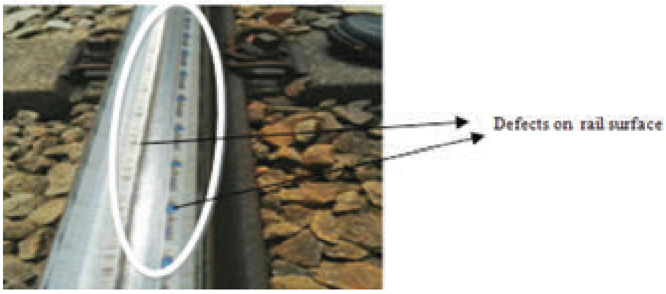

Figure 1: RCF defect of R260 at LRT

Solazzi & Mazzoni *et al.* (2023) reports that this hotspot is where the most stress happens on the component, enabling the formation of defects, cracks and the subsequent development to failure if the component is not well-designed and has not undergone the right durability assessment. For that reason, plenty of studies usually completes laboratory experiments by the manufacturer as to provide assessment reports in accordance with the standard ASTM to increase confidence when using its parts and it is making sure safe in the environment. Teng *et al.* (2022) conducts a laboratory experiment using the S-N curve to determine the characteristics of material either in terms of its vibration fatigue to verification.

Nowadays, it has lacking data on fatigue strength of R260 material. Nevertheless, a recent study of experimental fatigue life report of Gurubaran *et al.* (2017) that on the results of fatigue life for rail steel which is presented insufficient to consider their findings as used the stress ratio R= 0.1 to plot out the S-N curve, however instead to use R=-1 as principal in fatigue phenomena includes they do not apply the guidelines yet to divide the ratio to loading level to claim the safety loads and does not to reveals the way to obtain the mechanical properties (Dowling *et al.,* 2020). Their findings are less accuracy and less confident to use the way to address fatigue life. To tackle this methodology gaps, it is mandatory to obey the international standard of ASTM E8 and ASTM E466-15 regulation to set the experiment of fatigue life and to follow FKM guidelines in order to identify infinite level and safe loads. The importance of this, to ensure results correctly and properly valid as common practise for determining fatigue properties on S-N curve. In addition, to obtain fatigue life under the experiment, basic uni-axial fatigue testing apply the frequency of 10 with seven different loading level. As main objective of this research paper to investigate the fatigue failure of the sampled rail through an experiment using a Servo-Pulser fatigue machine to establish the S-N curve for the R260 rail profile. The particular significance of this study is to creating a fatigue strength record in the R260 steel database and it able to use for future reference in terms of material selection.

The work processes of this paper are organised as follows: In section 2, provides a way to set up the experiment and type of material adopts in railway. In section 3, it reveals the findings regard R260 rail specimen on mechanical properties and total fatigue life. Finally, section 4 conclusion on the overall research.

2.0 SETTING OF EXPERIMENTAL

A details study to define the fatigue life of R260 material specimen correctly with following to standard of American Society for Testing and Materials as well as recognized international body that develop technical standard for a material. It need to fulfil the some series of processes to obtain the accurate result. The Figure 2 displays the flow chart of experimental to complete this research since begins until end. As to reduce and avoid the serious injuries and illness in conducting experiment, the author(s) mandatory to concur and have obey guidelines and practice of laboratory safety handbook - Kuala Lumpur University includes to wear the proper personal protective equipment (PPE) such as safety glasses, gloves, lab coat, safety boots and particular regulations in the handbook for machining process, tensile testing and uniaxial fatigue testing.

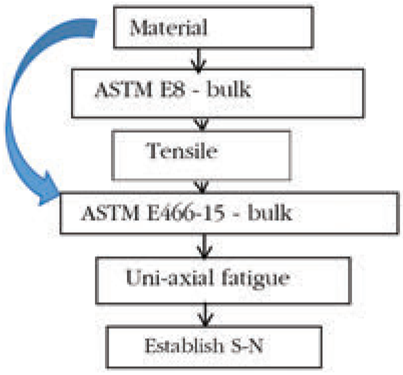

Figure 2: Flow chart of experimental

Figure 3(a): R260 material specimen

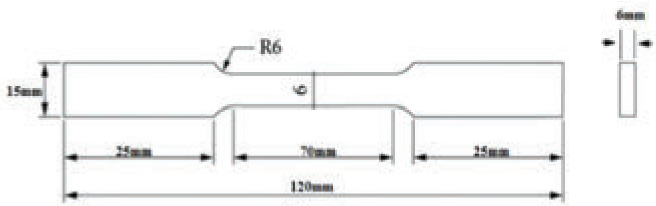

Figure 3(b): Dimension for tensile strength ASTM E8

2.1 Material Specimen

The material specimen provides through on behalf of the railway company as shown in Figure 3(a). The dimension was 7 cm x 5 cm as actual geometry. This rail profile of R260 was recognised in accordance Government of Malaysia in terms of regulation and manufacturer. The weight designed was 60 kg/metre (Azmalea, 2024). The material specimen can be divided into two pieces as the half piece for tensile and half piece for fatigue testing in order to saves material specimen.

2.2 ASTM E8

In order to determine the mechanical properties, the CNC machine was adopted to cut off the material specimen into some specimens as same shaped dimension of ASTM E8. The tolerance dimension to this specimens testing as in Figure 3(b).

2.3 Tensile Testing

Three specimens were used to find out the mechanical properties in tensile testing and the preparation specimens as of Figure 4(a). The Universal Tensile Machine less 100 kN have been utilized with following regulation ASTM E8 at room temperature as in Figure 4(b). The specimens subjected in axial and longitudinal forces. The forces applied on to specimen until certain deformation occur which lead to failure.

2.4 ASTM E466-15

To complete uniaxial fatigue testing, Lee *et al.* (2012) suggest to utilize the FKM guidelines that considers about some aspects such as survival rate, size correction factor and gradient factor in order to complete the uni-axial fatigue testing as Table 1 to determine the endurance limit withstand no breaking under cycling loading and to assist in dividing number of the stress ratio (R) as minimum and maximum. In this case, the R representatives as the ratio of the minimum to maximum happening in one period of a cycle as known in fully reversed in constant stress. The important to use R=-1 as set up the mean value of 0 to determine the highest loading and non-loading amplitude in form of tension-compression forces (ASTM E466-15). The advantage of R=-1 mostly adopt in myriad perspectives of the fatigue failure in S-N curve analysis

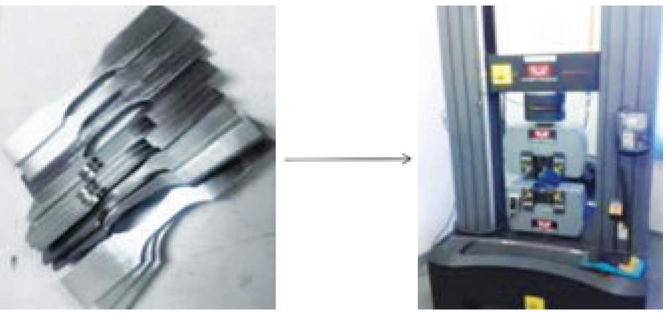

(a) *(b)*

Figure 4(a): Prepares specimens
(b): Universal Tensile Machine

Table 1: FKM guidelines parameter of uniaxial fatigue testing

No.	List of Considerations
1	C_R=0.843(97.5% Survival rate) - reliability factor
2	C_D=1.0 (Steel) - size correction factor
3	Gradient factor = 0.4
4	Normal temperature - 36.5^0c

to answer the perpendicular to the loading direction either in two axis or three axis (ASTM E466-15). Some pieces of material specimen was cut off to same shape following ASTM E466-15 as can see in Figure 5(a) and (b). It requires eighteen specimens to determine the fatigue properties of R260. The dimension was 120 mm x 25 mm x 3 mm. It have polishes to all specimens to make sure no crack, no defect and no corrosion with using sand paper grid 200 in order to well perform in fatigue testing (ASTM E466-15).

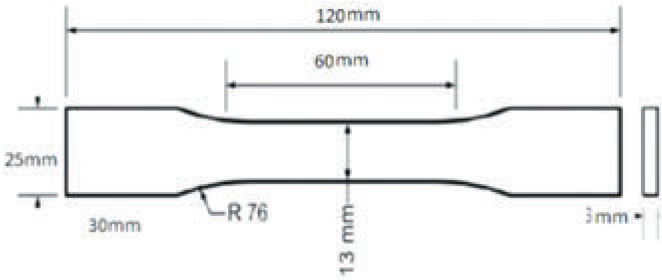

Figure 5(a): Dimension of ASTM E466-15

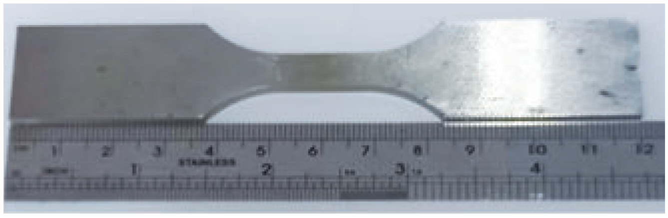

Figure 5(b): Real specimen

2.5 Uni-Axial Fatigue Testing

The Servo-Pulser less 100 kN was using to conduct the uni-axial fatigue testing. A sinusoidal waveform was applied of f=10Hz. A set of seven different loading used to investigate the fatigue life of 20%, 30%, 35%, 40%, 45%, 55%, 65%. Moreover, the 1.3 million cycle to failure have been setting on fatigue machine and the specimens break into two pieces surfaces considered failure. The self-adjustment of grips up and down to alignment the specimen in proper position 900. The fatigue life be gained on the experiment based ASTM E466-15. To address the categorize of fatigue life of material, three types of categorizes have been used such as low cycle fatigue (LCF) below 1000 cycle, above than 1000 until 106 as high cycle fatigue (HCF) and over than 107 fall into the endurance limit as infinite level as no break off on specimen and below the yield point.

3.0 FINDINGS

3.1 Mechanical Properties

Table 2 displays the mechanical properties obtained from the R260 rail specimens and specimens fracture as in Figure 6. The UTS and yield stress contribute highest value to compare with normal steel, cast iron and carbon steel (Dowling *et al.,* 2020). A number of UTS value for three specimens do not have significant different as in Table 3 and it is not essential to consider the effect of load correction factor caused of UTS value above than 1000 MPa (Lee *et al.,* 2012). The mean value of UTS represented to whole this experiment. However, the values of UTS have different due of some factors includes material surface effect in machining process, unnew material and the error in experiment may possible cause the speed of machine during to capture the tension process when neglected about machine capacity as uncertain to use the standard load application velocities.

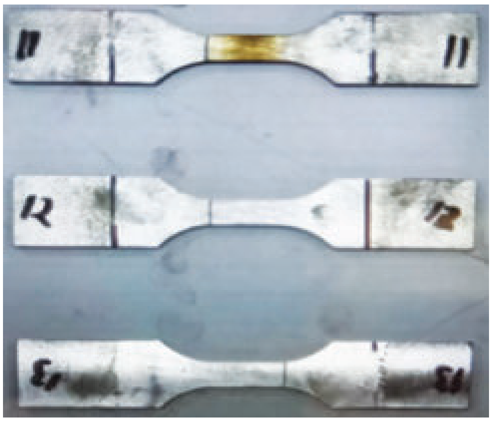

Figure 6: Specimens fracture under tensile testing

Table 2: Results of tensile strength

No. of specimen	Ultimate Tensile Strength (MPa)	Yields Stress (MPa)	Break Elongation
1	1167	1080	0.040
2	1145	1035	0.045
3	1125	1020	0.047

Table 3: Stress-strain curve of R260 for tensile strength

Area [mm²]	UTS [MPa]	Modulus [GPa]	Yield stress [MPa]	Break elongation [mm/mm]
24.000	1145	206	1035	0.045

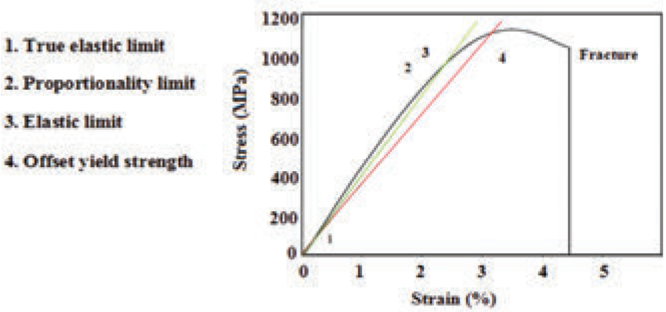

3.2 Fatigue Properties

Figure 7 shows that the specimens run till break off and Figure 8 demonstrates that specimens' failures of cycling loading with different stresses level. Following the Figure 9 demonstrates that stress-cycle (S-N curve) for the R260 material behaviour and key data to plot the S-N curve in Table 4. This data was falling the primary data as origin specifically in accordance standard ASTM E8 and ASTM E466-15. The trend on the stress amplitude and total number of fatigue life that 65% fall into LCF regime, 35%, 40%, 45%, 55% fall into HCF regime and 20% and 30% fall into endurance limit. To validate this data, the trend of curves for steel with previous work were compared in the range 102 until 107 as in Figure 9. The material type of R260 is stronger than normal steel as highest trends and good ability to withstand high stress curve. Therefore, it has potential to use for long term period due of good in return of investment based on performance.

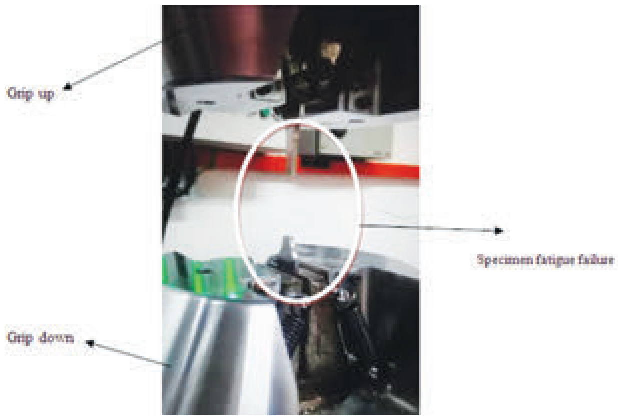

Figure 7: Specimen breaks

(a) 20% stress level - infinite

(b) 30% stress level - infinite

(c) 35% stress level

(d) 40% stress level

(e) 45% stress level

(f) 55% stress level

(g) 65% stress level

Figure 8: The specimens' failures of cycling loading with different stresses

The similar pieces of work in the context of fatigue life topic may compare to recent publication in terms of S-N curve trend is prepared of Kim *et al.* (2022). The fundamental to study the S-N curve salient to create the database for material as could help to decide in material selection through performance of any single material type in the future research. In their study, the main type material as made from aluminium alloy and it is set up of myriad different stress ratio (R) in reviewing for high cycle fatigue life. To verify the S-N curve behaviour that a number of stresses level influences the number of Nf cycle fatigue life. In Figure 9 regards the S-N curve trend as similar and it can be accepted and used for research (Kim *et al.,* 2022; Teng *et al.,* 2022).

The limitation of this research is a material specimen is unnew to obtain the real total fatigue life as given free of charge on behalf of urban railway for academic purpose.

It have diminished the ability of specimens to estimate the fatigue life. Besides, this experimental approach is focused on the uni-axial fatigue testing as suitable to find out the fatigue properties for tackling the RCF defects on rail surface nor represent to all points of defects in RCF propagation to become fatigue failure. It is pivotal to underline that the data on uni-axial fatigue is mandatory to compare with multi-axial fatigue in order to develop strong foundation as privilege to select stronger material for maintenance program. In future research, it is highly to recommend to increase a number of specimen for tensile testing and to be coating the rail specimen in order to review the longevity on fatigue life and it increase the strength of material.

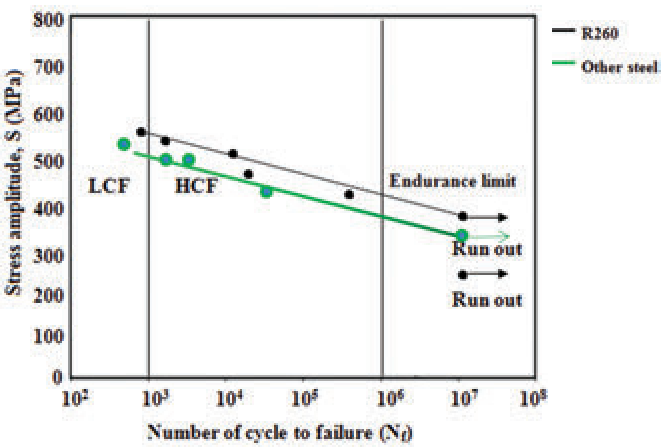

Figure 9: S-N curve of R260 versus other steel

Table 4: Data of testing for fatigue life

1	20%	5.498	-1	Passed	Infinite
2	30%	8.247	-1	Passed	Infinite
3	35%	9.6215	-1	Failure	871164
4	40%	10.996	-1	Failure	33919
5	45%	12.371	-1	Failure	33563
6	55%	15.119	-1	Failure	2923
7	65%	17.868	-1	Failure	996

4.0 CONCLUSIONS

This research is presented regard the total fatigue life for R260 rail specimen. The requirement and protocol of American Society for Testing and Materials-E8 have been fulfilled to determination the mechanical properties as of ultimate tensile strength, elongation and yield stress using tension-tension force in condition of room temperature 36.5^{0}C through three specimens evaluation separation in tensile testing. To address the S-N curve, the uniaxial fatigue testing was successfully applied to the specimens with seven different loading below UTS for examining the variation of stress level and important to observe fatigue strength characteristics, respectively. The findings shown that the 20% and 30% loading level fall into endurance limit as above than 10^7 withstand never break to fatigue failure, and 35%, 40%, 45% fall into high cycles fatigue (HCF) regime as above 10^4 number cycle to failure and 55% and 65% fall into low cycles fatigue (LCF) regime as below 10^4 and it has well compared with the other steel on the S-N curves and trends. It can be mentioned that R260 is strong material and good fatigue strength as can sustain for long term period. The benefits of this implications highlights the fatigue properties on material R260 though S-N curve and it can be used for validation databases of steel material.

5.0 ACKNOWLEDGMENTS

Support for this research was provided under Fundamental Research Grant Scheme (FRGS/1/2020/TK0/UNIKL/02/2), Malaysia's Ministry of Higher Education and most grateful to Kevin Rayment and team from Network Rail, UK for supporting training in railway engineering. ■

REFERENCES

[1] Tawfik, M.N., Padzi, M.M., Abdullah S., Hapaz., H., Zahar, M., & Firdaws, M. N. (2022). Approaches of Finite Element Analysis to Study Fatigue Analysis of Rail-Wheel Contact for Light Rail Transit. International Journal of Integrated Engineering, 14 (8), 86–91.https://doi.org/10.30880/ijie.2022.14.08.011.

[2] Interview with Tuan Haji Azmalea by M.N.Tawfik on Rail defects (Ampang, 2024).

[3] Putra, T.E. (2016) Improving the Fatigue Life Prediction of Automotive Components Using Simulated Strain Signal Methods, [Doctoral dissertation, Universität Duisburg-Essen. https://https://duepublico2.uni-due.de/servlets/MCRFileNodeServlet/duepublico_derivate_00042286/Putra_Diss.pdf.

[4] Gurubaran, P., Afendi, M., Nur Fareisha, M.A., Abdul Majid, M.S., Haftirman, I., & Rahman, M.T.A. (2017). Fatigue life investigation of UIC 54 rail profile for high-speed rail, IOP Conference Series. Journal of Physics: ICADME Conference Series 908012026, Shenzhen, China, 1-7. https://doi.org10.1088/1742-6596/908/1/012026.

[5] Tawfik, M.N., Padzi, M.M., Abdullah S., Harmanto D., Firdaws, & M. N, Hapaz H. (2022). A Review of the rolling contact fatigue of rail wheels under various stresses, Journal of Failure Analysis & Prevention, 23, 16–29. https://doi.org/10.1007/s11668-022-01568-6.

[6] Calcada, R. & Kaewunruen, S.(2022) Rail infrastructure iesilience: A best-practices handbook (Woodhead Publishing Series in Civil and Structural Engineering).

[7] Teng, Y., Liyang, X. & Hongyuan, Z. (2022). Experimental study on vibration fatigue behavior of aircraft aluminum alloy 7050, MDPI, Materials, 15(21), 7555, https://doi.org/10.3390/ma15217555.

[8] ASTM E466-15 (2015). Standard practice for conducting force controlled constant amplitude axial fatigue tests of metallic materials, ASTM International.

[9] Kim, H. S., (2022) A practical procedure for predicting the remaining fatigue life at an arbitrary stress ratio.

Journal of Composites Science, 6(6), 1-14. http://dx.doi.org/10.3390/jcs6060170.

[10] Shen, J. (2017). Responses of alternating current field measurement (ACFM) to rolling contact fatigue (RCF) cracks in railway rails, [Doctoral dissertation, University of Warwick, UK], 1-170. https://http://wrap.warwick.ac.uk/93593.

[11] Mazlan. S, Yidris. N, Koloor S.S.R., & Petru, M. (2020). Experimental and numerical analysis of fatigue life of aluminum AL 2024-T351 at elevated temperature, MDPI. Metals, 10(12),1-14. https://doi.org/10.3390/met10121581.

[12] Pereira, A.B., Fernandes, F.A., De Morais, A., Carvalhoso, P., & Morais, D. (2019) Development of a delamination fatigue testing machine for composite MDPI materials. Machines, 7(2), https://doi.org/10.3390/machines7020027.

[13] Solazzi, L. & Mazzoni, A. (2023) Experimental study of the fatigue life of off-highway steel wheels using the rim section test approach. Applied Sciences, 13(16), 1-19. https://doi.org/10.3390/app13169119.

[14] Tawfik, M.N., Padzi, M.M., & Abdullah, S., & Harmanto, D. (2023). Experiment and Smith, Watson and Topper model parameter to correlate fatigue life of rail steel. Research Square Platform, Preprint,1-11. https://doi.org/10.21203/rs.3.rs-3793055/v1.

[15] ASTM E8 (2024).Standard Test Methods for Tension Testing of Metallic Materials, ASTM International.

[16] Cini, A. (2012). Scribe marks at fuselage joints: initiation and propagation of fatigue cracks from mechanical defects in aluminium alloys, 1-298. http://dspace.lib.cranfield.ac.uk/handle/1826/7895.

[17] Dowling, N., Kampe, S., & Kral, M. (2020). Mechanical behaviour of materials: engineering methods for deformation, fracture and fatigue. Pearson.

[18] Lee, Y.L., Mark, E.B., & Hong, T.K. (2012).Metal fatigue analysis handbook: practical problem-solving techniques for computer-aided engineering, Elsevier. https://doi.org/10.1016/C2010-0-66376-0.

[19] Gren D., & Meyer K.A.,(2024) Effects of predeformation on torsional fatigue in R260 rail steel, International Journal of Fatigue, 179, 1-10, https://doi.org/10.1016j.ijfatigue.2023.108031. /C2010-0-66376-0.

[20] Padzi, M.M., Abdullah, S.M.N., & Harmanto, D.(2023). The prediction of fatigue failure analysis in simulation of UIC60 specimens of light rail transit with following ASTM E466-15, Kongzhi yu Juece. Control and Decision. 38(02), 887-892, https://www.kzyjc.org/article/the-prediction-of-fatigue-failure-analysis-in-simulation-of-uic60-specimens-of-light-rail-transit-with-following-astm-e466-15-standard-66376-0.

PROFILES

MN TAWFIK is former Chief Epiphron of Airbus Project of A319/A320/A321 in the Manufacturing of Aerospace for ORS/FRS/RIBS. His PhD major in vibration fatigue in railway closely collaboration training with Network Rail, UK for academic purposes. He received an MBA from London Met-Bucks New University, UK and he obtained a Professional Certificate in Energy Grid/Power System from Imperial College London, UK and completed a Diploma in Mechanical Engineering from Polytechnic Port Dickson.
Email address: nurtawfik27@gmail.com

MAHFODZAH MD PADZI is a senior lecturer in the Section Of Mechanical, Universiti Kuala Lumpur, MFI, Malaysia. She received her PhD. in mechanical engineering from UKM and an Masters Degree in Mechanical Engineering. She is registered with MBOT - Malaysia Board of Technologists since 2022. Her research interests include fatigue life assessment, vibration, engineering materials and NDT.
Email address: mahfodzah@unikl.edu.my

SHAHRUM ABDULLAH is a professor in the Department of Mechanical and Manufacturing Engineering, Universiti Kebangsaan Malaysia, Selangor, Malaysia. He received his PhD. in mechanical engineering from Sheffield University, United Kingdom. His research interests include fatigue life assessment, fracture mechanics, mechanics of materials signal analysis and engineering design.
Email address: shahrum@ukm.edu.my

DANI HARMANTO is an associate professor in the Aeronautical Engineering at the School of Engineering, De Montfort University, United Kingdom. He is vast experience in education sector more than 20 years. His research interests include finite element analysis, computational fluid dynamics and aerodynamics. He is Chartered Engineer (UK) and Fellow of Higher of Education, UK.
Email address: dani.harmanto@dmu.ac.uk

EFFECT OF DIFFERENT ADMIXTURES ON MECHANICAL PROPERTIES OF CONCRETE PAVING BLOCK: A COMPARATIVE STUDY

Asif Hossain Abir[1*] and Md. Akhter Hossain Sarker[2]

Abstract

Ever since their introduction nearly a century ago, concrete paving blocks have become increasingly common. They evolved into an alternative to burned clay brick and natural stone. Concrete paving blocks are used to lay down areas for vehicles and pedestrians as well. Durability is one of the most crucial elements in the production of high-quality concrete paving blocks. The aim of this study is to optimise the mechanical properties of concrete paving block units by experimenting with different admixtures. Compressive strength, water absorption, oven dry density, and drying shrinkage are among the attributes that were evaluated. The cost of production was also contrasted with and without the use of an admixture to achieve a comparable compressive strength. The results showed that admixtures could be used to produce high early strength units, and this was considered to be an economical factor in the production of concrete paving block units. At all ages, the use of admixtures increased these units' compressive strength by 30–40%. Although they did slightly increased density, additives also decreased the absorption and drying shrinkage of concrete paving block units.

Received: *20 August, 2024*
Revised: *10 September, 2024*
Accepted: *25 October, 2024*

[1]Senior Executive-Research & Development, Concord Ready-Mix & Concrete Products Ltd., Dhaka, Bangladesh.

[2]Principal Research Officer, Housing and Building Research Institute, Ministry of Housing and Public Works, Dhaka, Bangladesh.

****Corresponding author:***
asifhossain49@iut-dhaka.edu

Keywords:
Admixture, Compressive strength, Concrete paving block, Oven dry density, Production cost, Water absorption

1.0 INTRODUCTION

One material that is frequently used in the construction sector is concrete. It is made by combining the necessary amounts of cement, water, fine and coarse aggregates, and occasionally admixtures (Sudha & Bhikshma, 2024). Admixtures are a significant and increasingly common component of concrete mixes, even though they are not necessary like cement, aggregate, and water are Hu *at. Al* (2024) (Lo *et al.,* 2024). In fact, a mix without admixtures is now the exception in many countries. The ability of admixtures to provide concrete with significant physical and financial benefits is the cause of the significant increase in their use (Odeyemi *et al.,* 2024). Using concrete in situations where there were previously significant, or even insurmountable, challenges is one of these advantages. They also enable a greater variety of ingredients to be used in the mixture (Chen *et al.,* 2024). The survival of the concrete industry is largely dependent on the adoption of clever technical solutions to address the growing concerns about environmental pollution caused by construction materials and activities and the scarcity of natural resources, such as water. Admixtures are required in order to produce concrete with the proper design strength at a low water cement ratio due to the availability of a variety of cements other than regular Portland cement (Gandage, 2018).

Chemical admixtures are substances that are added to concrete in the form of powder or liquid to give it properties that aren't possible with standard concrete mixes (Williams *et al.,* 2020). Chemical admixtures are very little additions to concrete that are primarily used for air entrainment, water or cement content reduction, plasticization of fresh concrete mixtures, and setting time control (Allah *et al.,* 2024). Admixtures, while not always inexpensive, don't always mean spending more money because their application can save money on associated costs, such as labour costs for achieving compaction or increasing durability without the need for extra precautions (Hussain *et al.,* 2024). Nevertheless, it was found that chemical admixtures lower construction costs, alter the characteristics of hardened concrete, guarantee concrete quality while mixing, transporting, placing, and curing, and resolve specific emergencies during concrete operations (Ozturk & Engur, 2024). Admixtures composed of chemicals include water reducers, super plasticizers, set retarders, set accelerators, air entrainers, and specialty admixtures (Vilane *et al.,* (2021).

Chemicals known as additives are typically added to concrete to provide a variety of advantageous outcomes, including increased workability, enhanced strength and durability, acceleration, decreased void volume, improved plasticity, etc. (Ramachandran *et al.,* 2002). In comparison to the weight of all components and the overall composition of concrete, the composition of additives varies from 0.02% to 0.5% (Newman *et al.,* 2003). Retarding admixtures, according to the European

Federation of Concrete Admixture Associations (EFCA), work by influencing the hydration process, which lowers the rate at which water enters the cement particles and slows down the reaction rate (speed) between the cement and water (EFCA, 2006). On the other hand, certain admixtures have the ability to reduce water at a variety of dosages and, when used in large quantities, to speed up the concrete's compressive qualities. (ACI, 2004). On the other hand, certain admixtures have the ability to reduce water at a variety of dosages and, when used in large quantities, to speed up the concrete's compressive properties (SINTEF, 2007). Admixtures (retarders) for concrete setting time retardation can be inorganic (phosphates, borates, lead salts, etc.) or organic (lignosulphonates, hydroxycarboxylic acid, phosphonate, etc.). The quantity of water required to make the concrete more workable can be decreased by using a superplasticizer (Muhit, 2013). Long side chain polycarboxylic ether molecules improved fresh concrete performance, according to Sugamata *et al.* (2003) investigation into the effect of the chemical structure of polycarboxylic ether-based superplasticizer on fresh concrete performance. When superplasticizers are used with hardened concrete, the concrete becomes denser and has a higher compressive strength due to improved compaction effectiveness (Alsadey, 2015).

The type of cement used, the makeup of the fine and coarse aggregates, the concentration of the aggregates, the water quality used, the admixture type, and the ambient conditions—mostly temperature—all have a significant impact on the engineering properties of concrete (Özbayrak, 2024). Particles with sizes ranging from 75 µm to 4.75 mm are typically found in fine aggregate, while those with sizes ranging from 4.75 to 50 mm are found in coarse aggregate. The ease and uniformity with which fresh concrete can be mixed, transported, and compacted—without experiencing undue bleeding or segregation—is typically used to assess the quality of the material. (Neville, 1995). If the right amounts of fine and coarse aggregate are used, bleeding in newly mixed concrete can be minimized. Admixtures and a higher cement content can also aid.

Prior studies have demonstrated that the appropriate amount of admixtures can enhance the compressive strength of cement composite materials. According to (Akpokodje & Uguru, 2019), sandcrete blocks made with cassava waste water (as an admixture) had a 39% higher compressive strength than blocks made with fresh water. According to Sanjeev *et al.* (2019), concrete blocks' compressive and split tensile strengths increased when fly ash, ground granulated blast furnace slag (GGBS), and metakaolin were partially substituted for cement. According to Topçu and Ateşin (2016), when fresh concrete made with a naphthalenesulfonate-based admixture was compared to fresh concrete made with a lignosulfonate-based admixture, the slump flow results were better (better flowability). After 28 curing days, the compressive strengths of concretes made with modified polycarboxylic ether polymer (admixture) were found to be higher than those of concretes made with modified sulfonated polymer and synthetic polymer, according to a different study by Papayianni *et al.* (2005).

However, extensive research on mechanical properties of concrete paving block units by experimenting with different chemical admixtures was not conducted before. The aim of this study was to optimise the mechanical properties of concrete paving block units by experimenting with different admixtures. Compressive strength, water absorption, oven dry density, and drying shrinkage are among the attributes that were evaluated. The cost of production was also contrasted with and without the use of an admixture to achieve a comparable compressive strength.

2.0 MATERIALS

2.1 Cement

In this study, regular Portland cement (Local Brand) was utilised. It was brought into the lab and kept out of the rain. The chemical and physical characteristics of the cement are displayed in Tables 1 and 2 according to test results, the adopted cement complied with ASTM C150 Type I. (ASTM International, 1989b).

Table 1: Chemical composition and main compounds of cement

Oxide Composition	Abbreviation	Content Percent	Limits of ASTM C150 Type I
Lime	CaO	62.00	–
Silica	SiO2	21.70	–
Alumina	Al2O3	6.57	–
Iron oxide	Fe2O3	2.11	–
Sulphate	SO3	2.20	≤ 3.0%
Magnesia	MgO	2.90	≤ 6.0%
Potash	K2O	0.21	–
Soda	Na2O	0.15	–
Loss on ignition	LOI	1.11	≤ 3.0%
Insoluble residue	IR	0.85	≤ 0.75%
Lime saturation factor	LSF	0.90	–

Table 2: Physical properties of cement

Physical Properties	Test Results	Limits of ASTM C150 Type I
Specific surface area, Blaine method (m^2/kg)	274	280 (min)
Soundness (auto clave method)	0.31	0.8% (max)
Setting time (vicat's apparatus)		
Initial setting (minutes) Final setting (minutes)	112 217	60 (min) 600 (max)
Compressive strength		
3 days (N/mm2) 7 days (N/mm2)	21 27	12 (min) 19 (min)

2.2 Fine Aggregate

Throughout this work, nature sand with grading limits BS 882/1992 (British Standards Institute (BSI), 1992) and a maximum size of 4.75 mm was used. According to Table 3, the sieve analysis of the fine aggregate grading complied with BS 882/1992 (British Standards Institute (BSI), 1992). Table 4 shows the specific gravity, absorption, and sulphate content, all of which meet the same specifications.

Table 3: Grading of fine aggregate

Sieve Size (mm)	Cumulative Passing	Limits of BS 882/1992
4.75	100.00	89-100
2.36	82.68	60-100
1.18	76.00	30-100
0.60	61.43	15-100
0.30	39.81	5-70
0.15	13.49	0-15
Fineness modulus = 2.27		

Table 4: Physical properties of fine aggregate

Physical Properties	Test Results	Limits of BS 882/1992
Specific gravity	2.52	–
Sulphate content	0.18%	0.5% (max)
Absorption	2.32%	–

2.3 Coarse Aggregate

The maximum size of the crushed aggregate that was used was 10 mm. The coarse aggregate grading in Table 5 is in accordance with BS 882/1992 (British Standards Institute (BSI), 1992). Table 6 shows the specific gravity, sulphate content, and absorption of coarse aggregate.

Table 5: Grading of coarse aggregate

Sieve Size (mm)	Cumulative Passing	Limits of BS 882/1992
14.00	100	100
10.00	93	85-100
5.00	7	0-25
2.36	0	0-5

Table 6: Physical properties of coarse aggregate

Physical Properties	Test Results	Limits of BS 882/1992
Specific gravity	2.71	–
Sulphate content	0.07%	0.1% (max)
Absorption	0.86%	–

2.4 Admixture

This investigation employed two different forms of admixtures: i) polycarboxylate ether (PCE) and ii) lignosulfonate-based admixture. According to ASTM C494 Type F (ASTM International, 2006), polycarboxylate ether (PCE) is a light brown liquid with a long lateral chain that is free of chloride. This super plasticizer has a specific gravity of 1.05 at 25 degrees Celsius. It improves the strength, density, and workability of concrete, according to the earlier study. Using this high-range water-reducing admixture used in research, an efficient mixture can be created. PCE lowers water consumption by 15% to 20%. The lignosulfonate-based admixture has a specific gravity of 1.17 at 25 degrees Celsius and is a dark brown liquid that complies with ASTM C494 type C (ASTM International, 2006). Water demand is reduced by 5–10% when this admixture is used at a dosage of 0.3–0.6% (weight of cement). Figure 1 shows two different admixture used in this study.

(a) (b)

Figure 1: Two different admixture used in this study
(a) Polycarboxylate ether based superplasticizer
(b) Lignosulfonate-based admixture

3.0 MIX DESIGN

Several slump tests were conducted in compliance with ASTM C143 (ASTM International, 1989a) to determine the ideal admixture dosage that produces the greatest water reduction at the same workability and to adjust for the water content. According to these tests, the mix's maximum water reduction is 25%, which is equivalent to an admixture dosage of 1.5% by cement weight; water reduction stops at this dosage. Table 7 provides specifics about the mixes that were used in this investigation.

4.0 MIXING, CASTING AND CURING PROCEDURE IN FACTORY

In order to produce concrete paving block units, the experimental work was done in the Concord Ready-Mix and Concrete Products factory. Concrete's dry ingredients were added to the mixer to begin the material mixing process. To achieve a uniform mix, the materials were mixed for three minutes. After adding the necessary amount of water, the ingredients were thoroughly mixed for an additional three minutes. The admixture water content was deducted from the necessary amount of mixing water and the above procedure was applied to concrete. Concrete was mechanically moved from the mixer to the block-making machine using metal pans.

Table 7: Mix proportion of concrete paving block mixes

Mix Designation	Mix Ratio (Cement : FA : CA)	Water Content	Cement Content (kg/m3)	Type and Dosage of Admixture by Weight of Cement
Mix A	1:1.6:3	.48	395	-
Mix B	1:1.7:3.2	.36	395	1% Polycarboxylate ether based superplasticizer
Mix C	1:1.7:3.2	.32	395	1% Lignosulfonate-based admixture
Mix D	1:1.8:3.4	.36	395	1.5% Polycarboxylate ether based superplasticizer
Mix E	1:1.8:3.4	.32	395	1.5 % Lignosulfonate-based admixture

The blocks were placed inside the mold, which vibrated. The head and shoes were lifted out of the mold during the filling process to make room for the concrete. The head and shoes pressed against the top of the blocks when the mold was filled and vibrated. As seen in figure 2, they were moved down to extrude the blocks from the mold at the conclusion of the vibration period. Following that, an excavator is used to move the concrete paving blocks to the storage area for curing, as depicted in figure 3. Concrete paving block units were cured in the factory by being left in the storage area and, depending on the weather, being sprinkled with water. Curing period was 7 days. Figure 4 displays the final goods following the application of admixture.

Figure 2: After demolding from machine mold

Figure 3: Carrying to the storage place for curing

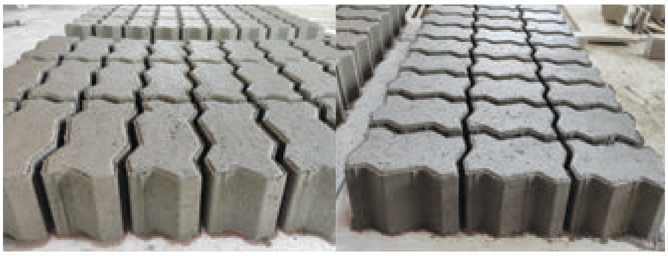

Figure 4: Finished products after the usage of admixture

5.0 TESTS RESULTS AND DISCUSSION OF EXPERIMENTAL WORK

5.1 Compressive Strength

The ASTM C140 was followed in the execution of this test (ASTM International, 2002). Table 8 and Figure 6 display the compressive strength of concrete paving block units for mixes with and without admixtures at various ages. The compressive strength of all units, both with and without admixtures, increases steadily with age. The compressive strength of the units increased to 45%, 49%, 35%, 46%, and 34% higher after 28 days of moist curing (sprinkled with water) than it was after three days for Mix A, Mix B, Mix C, Mix D, and Mix E, respectively. The units' compressive strength clearly increases as the amount of moist curing increases. When admixtures are used in the production of concrete paving block units, the factory curing time can be shortened because the finished units meet ASTM C90 (ASTM International, 1999), Grade-N1, requirements after just three days of moist curing. Mix A exhibits a lower compressive strength than mixes without admixtures, as demonstrated by the comparison with Mix B, Mix C, Mix D, and Mix E. This results from employing admixtures, which lowers the water content ratio. Even though pressed concrete is used to make concrete paving block units, the compressive strength of these units is increased by reducing the water content through the use of admixtures. Using these admixtures results in a roughly 30–40% increase in compressive strength for the produced concrete paving block units at all ages. Additionally, the use of admixtures gave the concrete paving block units that were produced an early strength, which could shorten the curing period. Mix B and Mix D, which contain superplasticizer based on polycarboxylate ether, have a lower compressive strength than Mix C and Mix E, which contain lignosulfonate-based admixture. It is also evident that a decrease in water content leads to an increase in compressive strength. Figure 5 displays the compressive strength testing of concrete paving block units.

Table 8: Compressive strength of hollow block concrete units

Mix Type	Compressive strength (MPa), at age (days)			
	3	7	14	28
Mix A	18.80	22.03	24.09	27.32
Mix B	24.09	28.79	31.73	35.84
Mix C	27.17	30.84	33.19	36.72
Mix D	25.35	30.58	32.99	37.10
Mix E	28.08	31.76	34.19	37.66

(a) (b)

Figure 5: Compressive strength testing of concrete paving block units
(a) compressive strength test setup
(b) typical rupture for a whole paving block

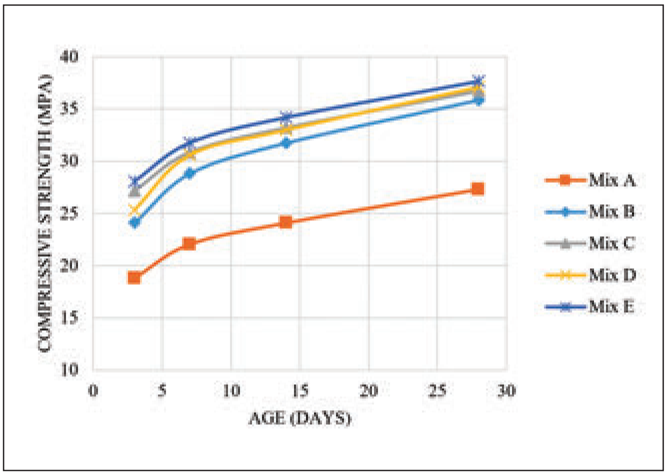

Figure 6: Development of compressive strength of different mixes of concrete paving block units with age

5.2 Absorption and Moisture Content

Table 9 displays the absorption and moisture content of concrete paving block units after 28 days of moist curing. These findings demonstrate that the use of admixtures reduces the absorption of concrete paving block units by lowering capillary porosity, which is brought about by a significant reduction in the water content ratio. Figure 7 shows the relationship between the concrete paving block units' compressive strength and absorption. Evidently, a reduction in absorption results in a rise in compressive strength. The moisture content results for each unit meet ASTM C90's type 1 (ASTM International, 1999) moisture-controlled unit requirements. Compared to Mix B and Mix D, which contain superplasticizer based on polycarboxylate ether, Mix C and Mix E, which contain lignosulfonate-based admixture, produce less absorption and moisture content. As the water content decreases, we can also see a decrease in absorption and moisture content.

Table 9: Absorption and moisture content

Type of Mix	Absorption (%)	Absorption (kg/m3)	Moisture Content (%)	ASTM C90
Mix A	5.70	126.92	36.10	Max. absorption 208 kg/m3
Mix B	4.13	100.70	28.50	
Mix C	4.04	93.10	29.45	
Mix D	4.07	96.71	29.07	
Mix E	4.01	90.44	29.74	

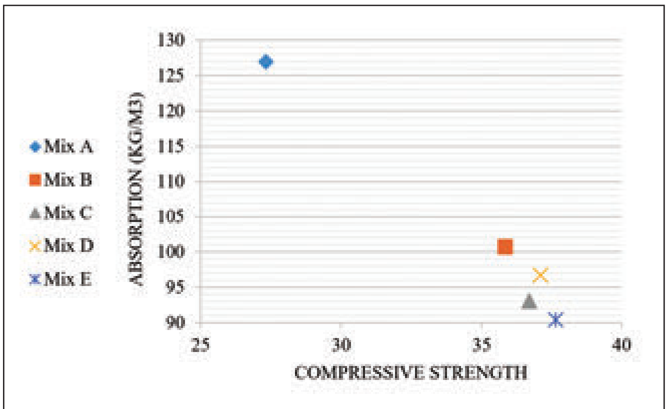

Figure 7: Relation between absorption and compressive strength for different mixes of concrete paving block units

5.3 Oven Dry Density

The ASTM C495 (ASTM International, 1985) was followed in determining the oven dry unit weight test. Table 10 lists the oven-dry density results at 28 days of age. Due to the admixture concrete's lower water content than the reference concrete, it is evident from the results that the units produced from Mix B, Mix C, Mix D, and Mix E (mixes containing admixtures) have a higher oven-dry density than units produced from Mix A. Figure 8 demonstrates how an increase in oven-dry density clearly raises a unit's compressive strength. Mix B and Mix D, which contain superplasticizer based on polycarboxylate ether, yield a lower dry density than Mix C and Mix E, which contain lignosulfonate-based admixture. We can also observe that dry density increases due to decrease in water content.

Table 10: Oven-dry density

Type of Mix	Oven-Dry Density (kg/m3)	Drying Shrinkage (%)	Percentage of Shrinkage Reduction (%)
Mix A	1543	0.028	–
Mix B	1565	0.016	43
Mix C	1579	0.012	57
Mix D	1569	0.015	47
Mix E	1585	0.011	60

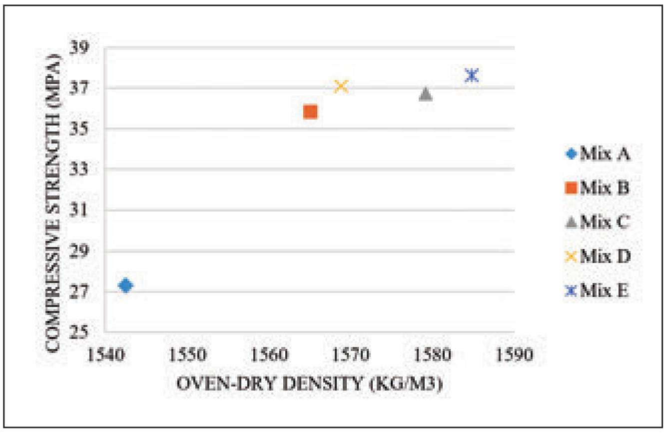

Figure 8: Relation between oven-dry density and compressive strength for different mixes of concrete paving block units

5.4 Drying Shrinkage

In accordance with ASTM C426 (ASTM International, 2002), this test was performed to ascertain the shrinkage of concrete paving block units. The drying shrinkage results for the concrete paving block units made with and without admixtures are displayed in Table 10. The findings demonstrate that the admixtures reduce drying shrinkage. This results from employing these admixtures to lower the percentage of water in the concrete. Additionally, by using these admixtures, the aggregate volume percentage is increased. It is well known that concrete with a higher aggregate content shrinks less. Mix B and Mix D, which contain superplasticizer based on polycarboxylate ether, exhibit greater drying shrinkage than Mix C and Mix E, which contain lignosulfonate-based admixture. We can also observe that drying shrinkage decreases due to decrease in water content.

5.5 Production Cost

Production cost of concrete paving block units decreased due to the usage of admixtures. By adding admixture high strength concrete can be produced. From this study it can be observed that, by adding admixture high strength concrete block was produced in spite of increasing aggregate ratio, which decreased the usage of cement and reduced the overall production cost of concrete paving block units. Table 11 shows the production cost of concrete paving block units for different mixes.

Table 11: Production cost of concrete paving block units for different mixes

Mix Type	Per Unit Price
Mix A	BDT 25.00
Mix B	BDT 23.50
Mix C	BDT 23.20
Mix D	BDT 22.50
Mix E	BDT 22.25

6.0 CONCLUSIONS

The results showed that by increasing the concrete paving block units' early age compressive strength, admixtures used in their manufacturing process enable a shorter curing time. Using admixtures results in a 30–40% increase in compressive strengths for the produced concrete paving block units at all ages. The use of admixtures lessens the absorption of concrete paving block units. Again, the oven-dry density of concrete paving block units is slightly increased by the use of admixtures. The drying shrinkage of the produced concrete paving block units is decreased by approximately 40–60% when admixtures are used. High strength concrete blocks were produced even with an increased aggregate ratio by adding admixture, which reduced the amount of cement needed and the overall cost of producing concrete paving block units. In future studies, the durability of the concrete paving block units' could be assessed.

7.0 ACKNOWLEDGEMENT

The authors would like to thank the technical staff in the concrete lab at the Housing and Building Research Institute for their support in conducting specimen testing and the technical staff of the factory of Concord Ready-Mix & Concrete Products Ltd. for precast unit production. ■

REFERENCES

[1] Akpokodje, O., & Uguru, H. (2019). Effect of fermented cassava waste water as admixture on some physic-mechanical properties of solid sandcrete blocks. International Journal of Engineering Trends and Technology (IJETT), 67(10), 216-222. Retrieved from https://www.researchgate.net/publication/337137032_Effect_of_Fermented_Cassava_Waste_Water_as_Admixture_on_Some_Physic-Mechanical_Properties_of_Solid_Sandcrete_Blocks

[2] Alsadey, S. (2015). Effect of superplasticizer on fresh and hardened properties of concrete. Journal of Agricultural Science and Engineering, 1(2), 70-74. Retrieved from https://www.researchgate.net/publication/336254043_Effect_of_Superplasticizer_on_Fresh_and_Hardened_Properties_of_Concrete

[3] Newman, J., John, B., & Choo, B. (2003). Advanced concrete technology: Constituent materials. Oxford : Butterworth-Heinemann.

[4] Papayianni, I., Oikonomou, N., Tsohos, G., & Mavria, P. (2005). Influence of superplasticizer type and mix design parameters on the performance of them in concrete mixtures. Cement and Concrete Composites, 27(2), 217-222. http://dx.doi.org/10.1016/j.cemconcomp.2004.02.010

[5] Vilane, B. R., Mbingo, S. R., & Innocent, S. M. (2021). The effect of calcium chloride admixture on the compressive strength of concrete blocks. Journal of Agricultural Science and Engineering, 7(2), 30-35. Retrieved from https://www.researchgate.net/publication/353081948_The_Effect_of_Calcium_Chloride_Admixture_on_the_Compressive_Strength_of_Concrete_Blocks

[6] ACI. (2004). Committee Report ACI 212.3R-04, Chemical Admixtures for Concrete. Michigan: American Concrete Institute (ACI) .

[7] Allah, S., Kassim , M., & Salman, G. (2024). The durability of concrete mortars with different mineral additives exposed to sulfate attack. Salud Ciencia y Tecnología - Serie de Conferencias, 3, 885. http://doi:10.56294/sctconf2024851

[8] ASTM International. (2006). Standard Specification for Chemical Admixtures for Concrete. West Conshohocken: ASTM International.

[9] ASTM International. (1985). ASTM C495 1985 Standard method for oven dry density of concrete. Annual book of ASTM Standards, 4(2).

[10] ASTM International. (1989a). ASTM C143 1989 Standards test methods for slump of hydraulic cement concrete. Annual book of ASTM Standards, 2(2), 85-86.

[11] ASTM International. (1989b). ASTM C150 1989 Standards Specification for Portland Cement. Annual book of ASTM Standards, 4(2).

[12] ASTM International. (1999). ASTM C90 1999 Hollow load-bearing concrete masonry units. Annual book of ASTM Standards, 4(2).

[13] ASTM International. (2002). ASTM C426 2000 Standard method for drying shrinkage of concrete block. Annual book of ASTM Standards, 4(2).

[14] British Standards Institute (BSI). (1992). BS 882/1992 Aggregate from natural sources for concrete. London: British Standards Institution.

[15] Chen, W., Wu, M., & Liang, Y. (2024). Effect of SF and GGBS on Pore Structure and Transport Properties of Concrete. Materials, 17(7), Liang. http://doi:10.3390/ma17061365

[16] EFCA. (2006). About Admixtures: Set Retarding. (European Federation of Concrete Admixture Associations) Retrieved 7 18, 2024, from https://www.efca.info/admixtures/set-retarding/

[17] Gandage, A. (2018). Admixtures in Concrete -A review. International Conference on Construction Real Estate Infrastructure and Project. Pune.

[18] Hu, B., Wang, X., Zhou, Y., Huang, X., & Zhu , Z. (2024). Seismic performance of shear-critical RC columns strengthened by multiple composites considering shifted failure zone. Case Studies in Construction Materials, 20, 1-21. https://doi.org/10.1016/j.cscm.2024.e02971

[19] Hussain, A., Wankhade, R., & Singh, H. (2024). Enhancing the properties of self-compacting concrete by using steel and polypropylene fibers. Practice Periodical on Structural Design and Construction, 29(3). http://doi:10.1061/ppscfx.sceng-1460

[20] Lo, H., Sutandar, E., & Budi, G. (2024). Study of the effect of mineral admixture addition on paving blocks' physical and mechanical properties. Jurnal Teknik Sipil, 24(2), 914. doi:10.26418/jts.v24i2.76545

[21] Muhit , I. (2013). Dosage limit determination of superplasticizing admixture and effect evaluation on properties of concrete. International Journal of Scientific & Engineering Research, 4(3), 1-4. Retrieved from https://www.ijser.org/researchpaper/Dosage-Limit-Determination-of-Superplasticizing-Admixture-and-Effect-Evaluation-on-Properties-of-Concrete.pdf

[22] Neville, A. (1995). Properties-of-Concrete-AM 149. 4th Edition. Essex: Addison Wesley Longman Ltd.

[23] Odeyemi, S., Anifowose, M., Oyeleke, M., Adeyemi, A., & Bakare, S. (2015). Effect of calcium chloride on the compressive strength of concrete produced from three brands of Nigerian cement. American Journal of Civil Engineering, 3, 1-5. http://doi:10.11648/j.ajce.s.2015030203.11

[24] Özbayrak, A. (2024). Experimental investigation of the relationship between dynamic characteristics and mechanical properties of fly ash-based geopolymer reinforced concrete beams. Journal of Materials in Civil Engineering, 36(8). http://doi:10.1061/jmcee7.mteng-17469

[25] Ozturk, Z., & Engur, M. (2024). Exploring the potential of slag waste generated after zinc metal recovery in geopolymer mortar production. Eskişehir Technical University Journal of Science and Technology A - Applied Sciences and Engineering. http://doi:10.18038/estubtda.1482349

[26] Ramachandran, V., Paroli, R. M., Beaudoin, J. J., & Delgado, A. H. (2002). Handbook of thermal analysis of construction materials (Chapter 4). New York: Noyes Publications.

[27] Sanjeev, N., Kumar, K. H., & Kumar, K. P. (2019). Strength and durability characteristics of steel fibre reinforced concrete with mineral admixtures. International Journal of Engineering and Advanced Technology (IJEAT), 9(1), 3893-3897. doi:http://dx.doi.org/10.35940/ijeat.A1223.109119

[28] SINTEF. (2007). Retarding admixtures for concrete state of the art. Trondheim: Sintef building and infrastructure. Retrieved from https://www.sintef.no/globalassets/sintef-byggforsk/coin/sintef-reports/sbf-bk-a07035_retarding-admixtures-for-concrete.pdf

[29] Sudha, V., & Bhikshma, V. (2024). Experimental investigation on field and laboratory curing of natural and recycled aggregate concrete. International Journal for Multidisciplinary Research, 6(3). doi:10.36948/ijfmr.2024.v06i03.16126

[30] Sugamata, T., Sugiyama, T., & Ohta, A. (2003). The effects of a new high-range water-reducing agent on the improvement of rheological properties. Seventh CANMET/ACI International Conference on Superplasticizers and Other Chemical Admixtures in Concrete. Berlin. Retrieved from http://worldcat.org/isbn/0870311271

[31] Topçu, İ. B., & Ateşin, Ö. (2016). Effect of high dosage lignosulphonate and naphthalene sulphonate based plasticizer usage on micro concrete properties. Construction and Building Materials, 120, 189-197. http://dx.doi.org/10.1016/j.conbuildmat.2016.05.112

[32] Williams, C. K., Al Hatali, E. M., & Al Ajmi, N. S. (2020). A study on the mechanical properties of concrete by partial replacement of cement with calcium chloride. International Research Journal of Engineering and Technology (IRJET), 7(8), 160-164. Retrieved from https://www.irjet.net/archives/V7/i8/IRJET-V7I825.pdf

PROFILES

ASIF HOSSAIN ABIR is the former Senior Executive, Research & Development Unit of Concord Ready-Mix & Concrete Products Ltd., Bangladesh. He graduated with the degrees of MSc. in civil engineering with a major in structural engineering in the year 2024 from Bangladesh University of Engineering and Technology and a bachelor of engineering in civil engineering in the year 2017 from Islamic University of Technology. Currently, he is actively engaged in research within the field of civil engineering, with a specific focus on green building materials, sustainable construction technology, and concrete products.
Email address: asifhossain49@iut-dhaka.edu

MD. AKHTER HOSSAIN SARKER is the former Principal Research Officer of Housing and Building Research Institute, Ministry of Housing and Public Works, Dhaka, Bangladesh. He has worked in sustainable construction technology and green building materials for thirty years. He received his M.Sc. in Geography from the Department of Geography at Jagannath College, which is part of Dhaka University, in 1987. He also received his B.Sc. (Hon's) in Geography from the same department in 1984. He is currently actively conducting research on concrete products, sustainable construction technology, and green building materials.
Email address: pro.hbri@gmail.com

ASSESSING RECREATIONAL FISHERIES ALONG THE KELANTAN COASTLINE FOR ENHANCING ENVIRONMENTAL RESOURCE MANAGEMENT

Ebrahim Al-Qadami[1], Mohd Adib Mohammad Razi[2*], Syed Muzzamil Hussain Shah[3], Mohamad Fahmi Mohamad Ideris[4], Mahran Mahamud[5]

Abstract

Recreational fisheries play a significant role in the cultural, social, and economic fabric of many communities worldwide. Proper management and conservation efforts are crucial to ensure the long-term sustainability of this sector and its associated economic benefits. Herein, recreational fisheries along the Kelantan coastline were explored to provide an in-depth overview on this sector aiming to develop proper management strategies. A site survey was performed between March and July 2020 to collect the primary data for this study. The results showed that the highest number of anglers was recorded during the daytime of the weekends with a percentage value of 83%, compared with 17% during the weekdays. In terms of bait, live shrimp, small fish, and squids were noticed to be the most commonly used bait, while the standard fishing gear used was rod-and-line. The total recreational fishing efforts amounted to 65,287 person-days/year, where 58.6 % was shore-based angling, while 41.4% was from boat-based angling with a total economic value of RM7.5 million/year. It is believed that the presented results offer valuable insight into the recreational fisheries along the Kelantan shoreline which help to understand the current situation and improve its sustainability and economic impact.

Received: *21 August, 2024*
Revised: *21 September, 2024*
Accepted: *22 October, 2024*

[1,2]Faculty of Civil Engineering & Built Environment, Universiti Tun Hussein Onn Malaysia, 86400 Parit Raja, Johor, Malaysia.

[1,2]Eco Hydrology Technology Research Centre (Eco-Hytech), Faculty of Civil Engineering & Built Environment, Universiti Tun Hussein Onn Malaysia, 86400 Parit Raja, Johor, Malaysia.

[3]Interdisciplinary Research Center for Membranes and Water Security, King Fahd University of Petroleum and Minerals, Dhahran, 31261, Saudi Arabia.

[4,5]Department of Irrigation and Drainage Malaysia, Coastal Division, Kuala Lumpur, Malaysia.

****Corresponding author:***
adib@uthm.edu.my

Keywords:
Angling, Economic impact, Environmental resources, Kelantan, Recreational fisheries

1.0 INTRODUCTION

Recreational fishing is the fastest-growing segment in the tourism industry, with a global annual growth rate of 5% (Patiyal & Pauline, 2023; Pita *et al.,* 2018; Zeelie, 2018). Its sustainability hinges on conservation-driven practices and the enforcement of regulations and management strategies designed to safeguard fish populations and their habitats (Soldo, 2022). Through catch-and-release, fish populations are preserved, and the overall health of ecosystems is maintained (Policansky, 2002). Regulations and management measures further prevent overfishing and ensure the long-term sustainability of fish populations which helps restore fish habitats, reduce pollution, and promote responsible angling practices (Methot Jr *et al.,* 2014). These efforts collectively contribute to minimising the environmental impact of recreational angling and ensure the long-term viability of recreational angling while minimising its ecological footprint (Cooke *et al.,* 2016).

Recently, recreational fisheries studies play a crucial role in enhancing environmental resource management by providing valuable insights into the interactions between human activities and natural ecosystems (Arlinghaus, 2006). These studies focus on understanding the dynamics of recreational fishing activities and their impact on marine and freshwater environments, as well as identifying strategies to mitigate negative effects and promote sustainable management practices (Lewin *et al.,* 2019). Recreational fisheries studies also examine socio-economic aspects such as angler behaviour, preferences, and spending patterns (Brown, 2016; Pita *et al.,* 2018). By understanding the motivations and preferences of recreational anglers, resource managers can create policies and regulations that effectively balance conservation goals with the needs and interests of the fishing community. Furthermore, economic analyses help quantify the value of recreational fisheries to local economies, providing policymakers with valuable information for decision-making and resource allocation (Hutt *et al.,* 2013; Toivonen *et al.,* 2004). Environmental resource management can also benefit from studies that explore the ecological impacts of recreational fishing practices. Research on habitat disturbance, bycatch, and the spread of invasive species can inform the development of regulations and management strategies aimed at minimising environmental harm.

Several studies have been conducted worldwide to investigate the recreational fisheries. For instance, Pérez-Bote and Roso (2014) conducted a survey investigating recreational fishing in rural areas of the South-Western Iberian Peninsula during the 2008-2009 fishing seasons. The survey highlighted that a significant portion of anglers engaged in fishing year-round or during the warmer months (37.43%), particularly on weekends and holidays. Shoreline fishing was the favoured method (89.47%), typically involving the use of natural bait (worms) either alone or in combination with artificial or live bait. Expenditure on equipment, permits, baits, and fuel displayed considerable variation, with some individuals spending between 100 and 300 euros per year (Pérez-Bote & Roso, 2014). Papadopoulos *et al.,* 2022 underscored the social and economic significance of marine recreational fishing in Greece. The study estimated that marine recreational fishers (MRF) constitute 7.93% of Greece's resident population, totalling an estimated 730,514 individuals. Primary fishing methods employed by MRF in Greece include shoreline fishing, boat fishing, and spearfishing. Annually, MRF in Greece undertakes approximately 11,461,765 fishing trips, resulting in a total catch of 9350 tons per year. The study advocates for meticulous planning and the implementation of a comprehensive management strategy, with a key component being the adoption of a licensing system covering all modes of marine recreational fishing (Papadopoulos *et al.,* 2022).

Malaysia has a rich history of fishing, whether for commercial purposes or leisure (Ahmad *et al.,* 2003) especially with the long coastal line the country has (Wan-Afnizan *et al.,* 2024; Yusoff *et al.,* 2024). Hoppy fishing in Malaysia took place in nearby ponds, rivers, disused mining pools, swamps, and rice fields inland, or in tidal lagoons and estuaries along the shoreline. These traditional practices have deep cultural roots and are essential to the Malaysian way of life, connecting angling to the cultural landscape of the majority of Malaysians (Abu Talib & Alias, 1997). While there is limited available data on angling in Malaysia, the activity holds strong traditional linkages and is deeply embedded in the cultural landscape of the country. The recreational fisheries along the Kelantan shoreline present an intriguing subject for investigation due to the lack of comprehensive understanding regarding the specific locations, levels of participation, and economic value associated with this activity. Identifying the gaps in current knowledge is essential for informed management and sustainable development of recreational fisheries in the region.

This paper focuses on the need to conduct a detailed study that systematically explores and analyses the various aspects of recreational fishing along the Kelantan shoreline, aiming to provide insights into its spatial distribution, participant demographics, and economic contributions. The present work is believed to cover the lack of detailed information on recreational fishing along the Kelantan shoreline, which will have direct implications for current management practices. Without a systematic study that explores the spatial distribution, participant demographics, and economic contributions of recreational fishing, managers may struggle to allocate resources effectively, plan sustainable development, or create policies that balance economic growth with environmental conservation. Inadequate understanding of these factors could lead to inefficient regulation, missed opportunities for tourism promotion, and potential environmental degradation due to poorly managed fishing activities.

2.0 METHODOLOGY

In the present study, recreational fisheries along the Kelantan state coastal area were investigated to understand the pattern, locations, and economic value of this sector. Figure 1 shows the location of the study area which extends from Thailand's southwest border to Terengganu state north prodder with a total shoreline length of 96 km. The study area was divided into five zones, namely (i) Reach 1 which extends between Pengkalan Kubur and Pantai Sri Tujuh areas, (ii) Reach 2 which extends between Pantai Sri Tujuh and Pengkalan Datu areas, (iii) Reach 3 which extends between Pengkalan Datu and Kemasin areas, (iv) Reach 4 which extends between Kemasin and Tok Bali areas, and (v) Reach 5 which extends between Tok Bali and Besut areas. The study area was divided into these 5 reaches following the concept of management unit (MU) which refers to a specific stretch of shoreline that shares similar characteristics in terms of natural coastal processes and land use. By grouping sections of the shoreline into MUs, planners can make decisions that are more tailored to the unique needs and behaviours of each specific section, ensuring better, more coherent management practices. This approach recognises that different parts of the coast may require different management strategies based on their characteristics.

Fisheries assessment along the study area was performed based on a site survey which was conducted on 13th-16th March 2020 and 20th-24th July 2020. The survey focused on collecting data about the locations of the recreational fisheries along the coastal area, accounting average number of anglers, and estimating the economic value of this activity. In the present study, the angling was divided based on the used method which includes shore-based angling and boat-based angling.

In terms of economic value, previous studies estimated RM50 payout per person-day, however, this estimation is clearly outdated. In the present study, for shore-based angling, RM100/day/anglers was estimated, while, for boat-based angling and according to the survey, the boats were rented out at RM1,200 to 1,500 for 10 anglers based on the angling location, which averages out at RM120 to 150/angler/ day.

Thus, in this study RM150/ angler/day was adopted for boat-based angling. To estimate the yearly economic value, firstly, the average number of anglers was estimated for each location for both weekdays and weekends. Secondly, the average time spent per angler was identified and according to the survey it was around 3 hours per day. Thirdly, the total person days were calculated by multiplying the number of anglers by the number of weekdays (261 each year) or weekends (104 each year) by 3 hours (the average angling time per day).

Figure 1:Study area and reaches boundaries

3.0 RESULTS AND DISCUSSION

3.1 Reach 1: Pengkalan Kubur to Pantai Sri Tujuh

For Reach 1, the site survey outcomes showed that the shore-based angling was mainly undertaken at Pantai Sri Tujuh, while the staging point for boat-based angling was at Kompleks LKIM Getting as shown in Figure 2. For shore-based angling, the activity was commonly undertaken during the weekends at which around 5-10 anglers were recorded undertaking the activity in the morning and increasing to about 15 anglers during the evening period. These observations are in agreement with the study conducted by Pérez-Bote and Roso, 2014 (Pérez-Bote & Roso, 2014). However, during nighttime, no fishing activities were recorded. During weekdays, only 3-5 daytime anglers were observed. Small shrimp, fishmeal, small fish, hermit crabs, and squid were used as bait. Normally, live bait (shrimps, small fish) were purchased from the aquarium shops at around RM0.50-RM1.00/individual, while fish, prawns, and squid were purchased at the wet markets for around RM5-RM10. The standard fishing gear used by anglers was noticed to be rod-and-line which costed around RM100-RM500. The survey showed that the most common species caught were Johnius spp., Mugil spp, Liza spp., Valamugil spp., Himantura spp., Gymnura spp., and Dasyatis spp. As for boat-based angling, there were 25 operators at Kompleks LKIM Geting. Rental rates were about RM1,500/day. Usually, recreational fishing is concentrated between March and November, especially during the weekends. However, no angling activities were undertaken during the monsoon season (December–February). Each boat could accommodate around 10 anglers/ boat. Even though there are 25 boats available for rental, only 5 trips (boats)/week were recorded. The main fishing gear used was rod-and-line with 3 to 5 rods per angler.

For boat-based angling, the average catch was estimated to be around 10 to 20 kg/boat. However, sometimes, the catch could exceed 100kg/boat, especially during the squid season. Overall, the investigation indicated that the total fishing effort amounted to 6,689 person-days a year, where 80.7% was contributed by boat-based angling and the remaining 19.3% by shore-based angling as listed in Table 1. The economic value of shore-based and boat-based angling was calculated by considering an average payout of RM100/person-day for shore-based angling and RM150/person-day for boat-based angling. Therefore, it can be found that the estimated direct financial value of recreational fisheries amounted to RM0.939 million per year for Reach 1 (refer to Table 1).

3.2 Reach 2: Pantai Sri Tujuh to Pengkalan Datu

Along Reach 2 coastal area, the highest number of shore-based angling was observed when compared with other reaches along the Kelantan shoreline. Shore-based angling was observed at four locations including Pengkalan Nangka Lagoon, Pantai Cahaya Bulan, Pantai Sabak, and Tanjung Kuala Sabak as shown in Figure 2. Pantai Cahaya Bulan recorded the highest number of shore-based anglers, especially on Fridays and Saturdays around 9.00 pm to 1.00 am. An average of 90 anglers were recorded undertaking the activities during this time frame. However, during weekdays, the numbers dropped drastically to only 3-5 anglers during the daytime and 7-10 anglers at nighttime. These observations in terms of angling during the weekdays and weekends are in agreement with the reported results by Pérez-Bote & Roso (2014) and Papadopoulos *et al.* (2022).

At the Pengkalan Nangka Lagoon, Pantai Sabak, and Tanjung Kuala

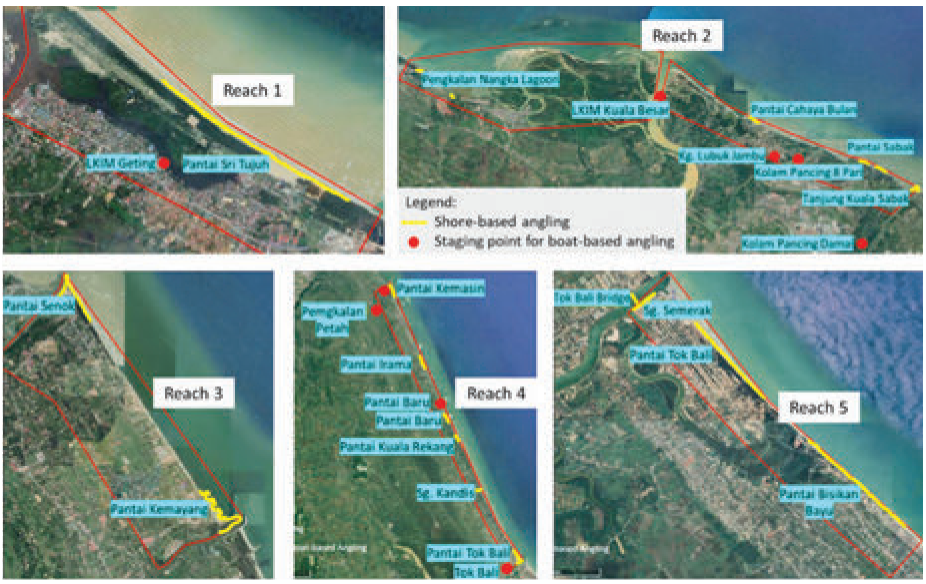

Figure 2: Locations of shore-based and boat-based anglings along the study area

Sabak, angling activities were only carried out during the daytime. At each location, approximately 3-5 anglers were observed during weekdays, however, the numbers increased to about 20-50 anglers during weekends at Pengkalan Nangka Lagoon and 20-30 anglers at Pantai Sabak and Tanjung Kuala Sabak. Most of the anglers spent about 3 hours/angling session. The most common bait used are live shrimp, small fish, shrimp, fishmeal, hermit crabs, and squids and the standard fishing gear used was rod-and-line. The best catch was reported to be obtained during the incoming tides, particularly springs, with catches ranging from 0.5-5 kg/person. Among the common species caught include the Alectis spp., Gnathanodon speciosus, Lates calcarifer, and Pomadasys spp.

In addition to shore-based angling, angling activities were also recorded at the recreational fee ponds located at Kg. Lapang Pari (Kolam Pancing 8 Pari) and Kg. Pulau Gajah (Kolam Pancing Damai) as shown in Figure 2. Around 20-50 anglers were noticed during weekdays, however, the number of anglers increased to around 80-100 anglers/day during the weekends at these fee ponds. The minimum angling hours are around 3 hours; however, some anglers could spend around 4-5 hours/entry. The entry fee is RM40 (3 hours) with an additional RM10 for the deposit and RM10/hour for subsequent hour for Kolam Pancing Damai and RM35 (3 hours) with an additional RM5 for the deposit and RM10/hour for an additional subsequent hour at Kolam Pancing 8 Pari. At Kolam Pancing Damai, the fish species stocked at the fee ponds are Lates calcarifer, Lutjanus argentimaculatus, Lutjanus spp., and Epinephelus spp., while at Kolam Pancing 8 Pari, only Lates calcarifer was noticed to be stocked.

Boat-based angling was also observed in this area, where the main staging point is at Kompleks LKIM Kuala Besar and Kg. Lubuk Jambu as shown in Figure 2. At Kompleks LKIM Kuala Besar, there were five outboard-powered boats available for rental. Rental rates were RM1,200/day. Recreational fishing was reported to be concentrated from March to November, especially during weekends, however, no angling activities were undertaken during the monsoon season (December – February). Each boat could accommodate around 10 anglers/boat. Angling is carried out at least 3-5 trips/week. The main fishing gear used was rod-and-line with 3 to 5 rods per angler. Anglers mainly used live fish and shrimp as baits and the main target species were Loligo spp., Lutjanus spp., Alectis indicus, Caranx ignobilis, and Alepes spp. The average catch was noticed to be about 10-20 kg/boat and sometimes, the catch could exceed 50kg/boat, especially during the squid season. Overall, the investigation indicated that the total fishing effort amounted to 31,065 person-days a year, where 44.7% is contributed by fee pond-based angling, followed by shore-based angling (33.6%), and the remaining 21.7% by boat-based angling. From the investigation, the total economic value for recreational fisheries in this area amounted to RM3.371 million per year as listed in Table 2.

Table 1: Recreational fishing effort at Reach 1 (Pengkalan Kubur to Pantai Sri Tujuh)

Location	Weekdays [a]	Weekends [b]	Total Person Days [c]	Unit Economic Value [d]	Economic Value (RM) [e]
Shore-based angling					
Pantai Sri Tujuh	4 anglers	23 anglers	1,289	RM100	128,900
Boat-based angling					
LKIM Getting	0 anglers	50 anglers	5,400	RM150	810,000
Total			6,689		938,900

*c = (a*3*261) + (b*3*104), e = c*d*

Table 2: Recreational fishing effort at Reach 2 (Pantai Sri Tujuh to Pengkalan Datu)

Location	Weekdays [a]	Weekends [b]	Total Person Days [c]	Unit Economic Value [d]	Economic Value (RM) [e]
Shore-based angling					
Pengkalan Nangka Lagoon	4 anglers	35 anglers	1,757	RM100	175,650
Pantai Cahaya Bulan	13 anglers	90 anglers	5,952	RM100	595,238
Pantai Sabak	4 anglers	25 anglers	1,367	RM100	136,650
Tanjung Kuala Sabak	4 anglers	25 anglers	1,367	RM100	136,650
Fee pond-base angling					
Kolam Pancing 8 Damai	35 anglers	90 anglers	6,936	RM100	693,563
Kolam Pancing Pari	35 anglers	90 anglers	6,936	RM100	693,563
Boat-based angling					
LKIM Kuala Besar	-	40 anglers	4,320	RM120	648,000
Kg. Lubuk Jambu		15 anglers	2,430	RM120	291,600
Total			31,065		3,370,913

*c = (a*3*261) + (b*3*104), e = c*d*

3.3 Reach 3: Pengkalan Datu to Kemasin

Along Reach 3 coastal area, only shore-based angling was recorded at two main locations, namely (i) Pantai Senok, and (ii) Pantai Kemayang as shown in Figure 2. The angling activity was mostly undertaken during weekends, where approximately 20-35 anglers were observed. During weekdays, only 5-10 anglers undertook the angling activity. The most common bait used was live shrimp, small fish, shrimp, fishmeal, hermit crabs, and squids.The standard fishing gear used by anglers was noticed to be rod-and-line. The most target species were Alectis spp., Gnathanodon speciosus, Lates calcarifer, and Pomadasys spp.

The total fishing effort at this location was estimated at 3,710 person-days per year, with a direct economic value of RM0.371 million as listed in Table 3.

3.4 Reach 4: Kemasin to Tok Bali

Along reach 4 coastal areas, both shore and boat-based angling activities were observed. Shore-based angling was recorded at Pantai Irama, Pantai Melawi, Pantai Kuala Rekang, Sg. Kandis and Pantai Tok Bali as shown in Figure 2. The angling activities were noticed to be undertaken during the daytime of the weekends only. At each location, there were 20-30 anglers, most of them spent around 3 hours/angling session. The most common bait used were live shrimp, small fish, and squids and the standard fishing gear used was rod-and-line. Among the common species caught from shore-based angling include the Johnius sp., Mugil spp., Liza spp., Valamugil spp., Arius spp., and Himantura spp.

As for boat-based angling, the staging points for boat rental were noticed to be at Kuala Kemasin, Pengkalan Petah, Pantai Baru, and Tok Bali as shown in Figure 2. The boats available for rental at Kuala Kemasin, Pengkalan Petah, and Tok Bali were inboard-powered boats, while at Pantai Baru, only outboard-powered boats were available. At Kuala Kemasin and Pengkalan Petah, the rental rate was around RM1,200/day, while RM1,500/day at Tok Bali. Each boat could accommodate around 10 anglers, and the average trips were reported to be between 3-5 trips/week. Recreational fishing was concentrated between March and November, especially during weekends however no angling activities were undertaken during the monsoon season (December – February). The main target species were Loligo spp., Lutjanus spp., Alectis indicus, Caranx ignobilis, Alepes spp., and Scomberoides spp. The angling hotspots were within Sg. Raja Gali and Sg. Kelantan as well as 5 nautical mile (nm) from the shoreline. In Reach 4, the total fishing effort was estimated at 19,723 person-days per year, with a direct economic value of RM2.432 million as listed in Table 4.

Table 3: Recreational fishing effort at Reach 3 (Pengkalan Datu to Kemasin)

Location	Weekdays [a]	Weekends [b]	Total Person Days [c]	Unit Economic Value [d]	Economic Value (RM) [e]
Shore-based angling					
Pantai Senok	7 anglers	30 anglers	1,855	RM100	185,513
Pantai Kemayang	7 anglers	30 anglers	1.855	RM100	185,513
Total			3,710		371,025

*c = (a*3*261) + (b*3*104), e = c*d*

Table 4: Recreational fishing effort at Reach 4 (Kemasin to Tok Bali)

Location	Weekdays [a]	Weekends [b]	Total Person Days [c]	Unit Economic Value [d]	Economic Value (RM) [e]
Shore-based angling					
Pantai Irama	-	25 anglers	975	RM100	97,500
Pantai Melawi	-	25 anglers	975	RM100	97,500
Pantai Kuala Rekang	-	25 anglers	975	RM100	97,500
Sg. Kandis	-	25 anglers	975	RM100	97,500
Pantai Tok Bali	-	25 anglers	975	RM100	97,500
Boat-based angling					
Kuala Kemasin	40 anglers		4,320	RM120	518,400
Pengkalan Petah	40 anglers		4,320	RM120	518,400
Pantai Baru	15 anglers		810	RM120	97,200
Tok Bali	50 anglers		5,400	RM150	810,000
Total			19,725	-	2,431,500

*c = (a*3*261) + (b*3*104), e = c*d*

Table 5: Recreational fishing effort at Reach 5 (Tok Bali to Kuala Besut)

Location	Weekdays [a]	Weekends [b]	Total Person Days [c]	Unit Economic Value [d]	Economic Value (RM) [e]
Shore-based angling					
Pantai Tok Bali	7 anglers	30 anglers	1,855	RM100	185,513
Pantai Bisikan Bayu	7 anglers	40 anglers	2,245	RM100	224,513
Total			4,100		410,025

*c = (a*3*261) + (b*3*104), e = c*d*

3.5 Reach 5: Tok Bali to Kuala Besut

Along Reach 5 only shore-based angling was observed at two locations, namely (i) Pantai Tok Bali (including Tok Bali Bridge and Sg. Semerak), and (ii) Pantai Bisikan Bayu as shown in Figure 2. The angling activity was mostly undertaken during weekends, where approximately 20-35 anglers were observed at Pantai Tok Bali (including Tok Bali Bridge and Sg. Semerak) and 30-50 anglers along the Pantai Bisikan Bayu. During weekdays, only 5-10 anglers were noticed to be involved in this activity. The most common bait used was noticed to be live shrimp, small fish, shrimp, fishmeal, and squids. The standard fishing gear used by anglers was rod-and-line. These observations are in agreement with the reported results by (Mike & Cowx, 1996).

The most target species were Johnius spp., Mugil spp., Liza spp., Valamugil spp., Himantura spp., Gymnura spp., and Dasyatis spp. In terms of economic value, Reach 5 contributed to the economy with a total amount of RM0.410 million each year which corresponds to 4100 person-day per year as listed in Table 5.

3.6 Comparison Between Shore-Based and Boat-Based Angling

Figures 3a and 3b show a comparison between shore-based and boat-based angling in terms of total person days and total economic value, respectively. Firstly, it can be noticed that for reaches 3 and 5 there was no boat-based angling and only shore-based angling was recorded. Secondly, it can be seen that the shore-based angling recorded the highest economic value at Reach 2 with a total amount of RM2,431,314 corresponding total which corresponds to 24315 total person days. On the other hand, boat-based angling recorded the highest economic value at Reach 4 with a total amount of RM1,944,000 which corresponds to 14850 total person days. Overall, both angling activities contribute to almost the same economic value in total at which the total economic values were found to be RM3,828,766 and RM3,693,600 for shore-based and boat-based angling, respectively.

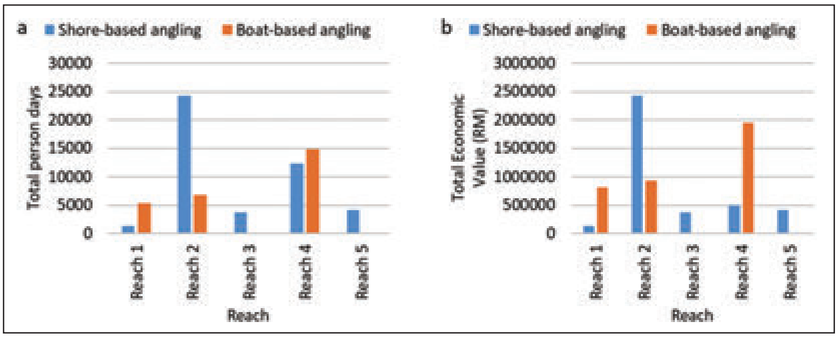

Figure 3: Comparison between shore-based and boat-based angling (a) total person days, and (b) total economic value

The present study's limitations, particularly regarding data and data collection methods, are important to acknowledge. Field surveys were conducted only during limited periods in March and July 2020, which introduces certain constraints, particularly related to seasonal variability. This seasonal limitation may affect the representativeness of the data. A key shortcoming is that the surveys did not cover the monsoon season (December-February), a time when no angling activities were observed. As a result, the study may not fully capture the annual dynamics of recreational fishing, potentially overlooking important seasonal fluctuations in angler participation and fish availability. To address these limitations, it is recommended that a long-term monitoring program be established. Such a program should take into account seasonal variations, particularly during the monsoon season, to provide a more comprehensive understanding of recreational fishing patterns and their broader ecological and economic impacts.

4.0 CONCLUSIONS AND SUMMARY

In the present study, recreational fisheries along the Kelantan shoreline were investigated through field survey which was conducted between 13th-16th March 2020 and 20th-24th July 2020. The study covered around 96 km shoreline length which was divided into 5 reaches including reach 1 (Pengkalan Kubur to Pantai Sri Tujuh), reach 2 (Pantai Sri Tujuh to Pengkalan Datu), reach 3 (Pengkalan Datu to Kemasin) reach 4 (Kemasin to Tok Bali), and reach 5 (Tok Bali and Besut). The results showed that there are two main types of angling in the study area, namely (i) shore-based angling, and (ii) boat-based angling. The angling activities were commonly concentrated during the daytime of the weekends where the highest number of anglers were observed. The average angling time is around 3 hours/day however the angling time could reach up to 5 hours. Furthermore, it was noticed that no angling activity during monsoon seasons (December- February). The survey showed that the most common bait used were live shrimp, small fish, and squids and the standard fishing gear used was rod-and-line. Recreational fisheries in Kelantan shoreline accounted for 45709 total person days/year with a total economic value of RM3,828,766/year for shore-based angling, while 27000 total person days/year and RM3,693,600 economic value for boat-based angling.

Overall, the recreation fisheries in Kelantan state coastal area accounted for a direct economic value of around RM7.5 million each year. The findings of the current study provide valuable insights into the sustainable management of recreational fisheries along the Kelantan shoreline. To ensure the long-term viability of this resource, several key recommendations are proposed, such as establishing a comprehensive, long-term monitoring program to track trends in recreational fishing activities and assess their impact on local fish populations and habitats. This program should include seasonal variations, with a particular focus on understanding the factors influencing angling during the monsoon seasons. Additionally, conducting ecological impact assessments to evaluate the ecological footprint of recreational fishing will contribute to the effective management of recreational fisheries in the Kelantan state coastal area.

ACKNOWLEDGMENT

This study was funded by the Department of Irrigation and Drainage (DID), Malaysia as a part of the Integrated Shoreline Management for Kelantan State under the 12th Malaysia Plan. Authors would like to thank the Malaysia Government through its implementing agency DID. ■

REFERENCES

[1] Abu Talib, A., & Alias, M. (1997). Status of fisheries in Malaysia-an overview. Status and Management of Tropical Coastal Fisheries in Asia. ICLARM Conference Proceedings, 53(208), 47–61.

[2] Ahmad, A. T., Salim, K., Chee, P. E., Isa, M. M., & Lim, C.F. (2003). An overview of the socioeconomic status of fisheries in Malaysia.

[3] Arlinghaus, R. (2006). Overcoming human obstacles to conservation of recreational fishery resources, with emphasis on central Europe. Environmental Conservation, 33(1), 46–59.

[4] Brown, C. J. (2016). Social, economic and environmental effects of closing commercial fisheries to enhance recreational fishing. Marine Policy, 73, 204–209.

[5] Cooke, S. J., Hogan, Z. S., Butcher, P. A., Stokesbury, M. J. W., Raghavan, R., Gallagher, A. J., Hammerschlag, N., & Danylchuk, A. J. (2016). Angling for endangered fish: conservation problem or conservation action? Fish and Fisheries, 17(1), 249–265.

[6] Hutt, C. P., Hunt, K. M., Steffen, S. F., Grado, S. C., & Miranda, L. E. (2013). Economic values and regional economic impacts of recreational fisheries in Mississippi reservoirs. North American Journal of Fisheries Management, 33(1), 44–55.

[7] Lewin, W.C., Weltersbach, M. S., Ferter, K., Hyder, K., Mugerza, E., Prellezo, R., Radford, Z., Zarauz, L., & Strehlow, H. V. (2019). Potential environmental impacts of recreational fishing on marine fish stocks and ecosystems. Reviews in Fisheries Science & Aquaculture, 27(3), 287–330.

[8] Methot Jr, R. D., Tromble, G. R., Lambert, D. M., & Greene, K. E. (2014). Implementing a science-based system for preventing overfishing and guiding sustainable fisheries in the United States. ICES Journal of Marine Science, 71(2), 183–194.

[9] Mike, A., & Cowx, I. G. (1996). A preliminary appraisal of the contribution of recreational fishing to the fisheries sector in north-west Trinidad. Fisheries Management and Ecology, 3(3), 219–228.

[10] Papadopoulos, A., Touloumis, K., Tziolas, E., Boulamatsis, D., & Koutrakis, E. (2022). Evaluation of marine recreational fisheries and their relation to sustainability of fisheries resources in Greece. Sustainability, 14(7), 3824.

[11] Patiyal, R. S., & Pauline, A. (2023). Livelihood Opportunities with Recreational Fisheries and Ecotourism. In Fisheries and Aquaculture of the Temperate Himalayas (pp. 433–440). Springer.

[12] Pérez-Bote, J. L., & Roso, R. (2014). Recreational fisheries in rural regions of the South-Western Iberian Peninsula: a case study. Turkish Journal of Fisheries and Aquatic Sciences, 14(1).

[13] Pita, P., Hyder, K., Gomes, P., Pita, C., Rangel, M., Veiga, P., Vingada, J., & Villasante, S. (2018). Economic, social and ecological attributes of marine recreational fisheries in Galicia, Spain. Fisheries Research, 208, 58–69.

[14] Policansky, D. (2002). Catch-and-release recreational fishing: a historical perspective. Recreational Fisheries: Ecological, Economic and Social Evaluation, 74–94.

[15] Soldo, A. (2022). An Assessment of Catches of Shore and Boat Recreational Angling along the Coast of the Adriatic Sea. Journal of Marine Science and Engineering, 10(12), 1999.

[16] Toivonen, A., Roth, E., Navrud, S., Gudbergsson, G., Appelblad, H., Bengtsson, B., & Tuunainen, P. (2004). The economic value of recreational fisheries in Nordic countries. Fisheries Management and Ecology, 11(1), 1–14.

[17] Wan-Afnizan, W. M., Al-Qadami, E. H. H., Razi, M. A. M., Aminon, N. A., Mahamud, M., & Aziz, A. (2024). Detection of mainland Kedah's shoreline changes (2013-2020); a case study. IOP Conference Series: Earth and Environmental Science, 1347(1), 12017.

[18] Yusoff, M. A. M., Al-Qadami, E. H. H., Razi, M. A. M., Wang, M., Daud, Z. H., Mokhtar, A., & Mahamud, M. (2024). Wave climate analysis for shoreline management plan in Kelantan, Malaysia. IOP Conference Series: Earth and Environmental Science, 1347(1), 12008.

[19] Zeelie, E. (2018). A critical analysis of the spending behaviour of recreational fishing in South Africa. North-West University.

PROFILES

EBRAHIM AL-QADAMI is a postdoctoral research fellow at the Faculty of Civil Engineering and Built Environment, Universiti Tun Hussein Onn Malaysia (UTHM). Dr. Al-Qadami obtained his Ph.D. from Universiti Teknologi PETRONAS (UTP) in 2022 and his master's degree from Universiti Putra Malaysia (UPM) in 2017. Dr. Al-Qadami does research on coastal engineering, flood risk modelling, urban stormwater management, and water resources management.
Email address: ebrahim@uthm.edu.my

MOHD ADIB MOHAMMAD RAZI is an associate professor at the Faculty of Civil Engineering and Built Environment, Universiti Tun Hussein Onn Malaysia (UTHM), and the head of the Eco Hydrology Technology Research Centre (Eco-Hytech). He obtained a PhD in Civil Engineering from Universiti Teknologi Mara, Malaysia. He is a registered professional engineer with the Board of Engineers, Malaysia. Ap. Ir. Dr. Mohd Adib Mohammad Razi does research on coastal engineering, flood risk modelling, urban stormwater management, hydraulics, and hydrology.
Email address: adib@uthm.edu.my

SYED MUZZAMIL HUSSAIN SHAH is a postdoctoral research fellow at the Interdisciplinary Research Center for Membranes and Water Security, King Fahd University of Petroleum and Minerals. Dr. Shah obtained his master's and Ph.D. from Universiti Teknologi PETRONAS (UTP) in 2014 and 2019. Dr. Shah is a member of the Pakistan Engineering Council, Institute of Engineers - Malaysia, American Society of Civil Engineers, Australian Water Association, and World Society of Sustainable Energy Technologies.
Email address: syed.shah@kfupm.edu.sa

MOHAMAD FAHMI MOHAMAD IDERIS is the Principal Assistant Director at the Coastal Zone Management Division, Department of Irrigation and Drainage (DID) Malaysia. He obtained bachelor's and master's degrees in civil engineering, specializing in sustainable water resource engineering from Universiti Kebangsaan Malaysia (UKM). He is a Registered Professional Engineer (P.Eng.) with the Board of Engineers, Malaysia (BEM), and a corporate member of the Institution of Engineers, Malaysia (MIEM). Ir. Ideris is also a member of the Malaysian StormWater Organisation (MSO) and the Malaysian National Committee on Irrigation & Drainage (MANCID).
Email address: mfahmi@water.gov.my

MAHRAN MAHAMUD is a Chief Assistant Director at River Basin Management Division, Department of Irrigation & Drainage. He has been working in the Coastal Zone Management Division for several years and obtained a Master's in Civil & Structural Engineering in 2016 from Universiti Kebangsaan Malaysia. He is a registered professional engineer with a practicing certificate from the Board of Engineers, Malaysia. Ir Mahran has managed and supervised several coastal management studies and detailed designs.
Email address: mahran@water.gov.my

MANUSCRIPT PREPARATION GUIDELINES FOR IEM JOURNAL AUTHORS

The aim of publishing the Journal of the Institution of Engineers Malaysia (or IEM Journal) is to promote the advancement of science, engineering, and technology; disseminate new and current knowledge; share novel findings among practising engineers, researchers and other interested colleagues. Hence, the IEM Journal covers a wide range of practical and diversified engineering disciplines, including publishing papers on any subjects relevant to the engineering and technology of today. As in other journals, all paper submissions to the IEM journal will be peer-reviewed by professionals.

Submission of a contribution is taken to manifest the fact that the submission has not been submitted, accepted, published, or copyrighted elsewhere. To avoid publication delays, please send all manuscripts to the Editor (via the Online Journal Submission) and observe the following guidelines. Each paper is independently peer-reviewed.

Types of Papers

IEM Journal will accept any submissions that fall within the three types of papers shown below:

- **Research Paper**

Significant research and development or applications in any field of engineering and/or technology. Submissions should be about 8-14 pages.

- **Review Paper**

Articles which summarises the state-of-the-art of a specific area of research. Submissions should be about 10-20 pages.

- **Brief Paper**

A concise description of new technical concepts or applications within the scope of the journal. Submission should be about 4 pages

Together with the paper submission, at least four (4) reviewers complete with their contact details (official postal and email address, and telephone number) are to be proposed by authors. Reviewers should be the experts in their research areas.

Plagiarism Policy

IEM Journal strictly prohibits any form of Plagiarism.

If the manuscript has been presented, published, or submitted for publication elsewhere, please inform the Editor. Our primary objective is to publish technical materials not available elsewhere.

Format and Elements of Submitted Texts

a) Initial Submission

For initial submission and reviewing, ALL papers are accepted regardless of the formatting used.

b) Final Submission

Upon final submission of paper, authors are required to follow the manuscript instruction guidelines and paper template as presented below.

Please prepare your main text document in Microsoft Word and PDF format, text should be single line spaced, line numbered and pages should be numbered. You can download the paper template here.

Please note that the style that you submit your paper in (e.g. any additional italics or bold fonts, bullet points, etc.) may be changed on publication to accommodate our publication style.

Manuscript Style

Language:

- The language of the IEM Journal is in English. However, a paper in Bahasa Melayu is also accepted. For accepted papers, an abstract in English and Bahasa Melayu must be included.
- The manuscript should be able to be readily understood by an engineer and researchers alike and should avoid any colloquialisms.
- The terms, including nomenclature and abbreviations, and style should be consistent throughout your journal paper. If you collaborate with other writers, please communicate clearly with them.
- Avoid referring directly to the names of individuals, organisations, products, or services unless essential to the comprehension of the manuscript. Gratuitous flattery or derogatory remarks about a person or organisation should not be included.
- Symbols and Units: SI and derived units should be used, if possible.
- Abbreviations: the use of internationally recognised abbreviations is allowed in the text. The abbreviations should be defined on first use. Abbreviations should not be used in the title.

Manuscript Guide

The following is a detailed manuscript preparation guide for articles submitted to IEM Journal; however, they can, in the most part, be used as a basis for other article types amending to concur with the page limit and premise of the formats, as appropriate.

The manuscript should be typewritten using single-spacing, font of 12 Times Roman; on one side of sheet only and in a single column format.

Title

Titles are limited to 150 characters, including spaces. Please avoid the use of any abbreviations, acronyms, or formulae. Titles should clearly reflect the content of the manuscript and any search terms that readers may use should be considered and incorporated.

List of Authors Name

List down all the names of authors (who has contributed to the paper) and the respective affiliations. From the list of authors, place an asterisk (*) next to the corresponding author's name. Provide an official email address of the corresponding author. **Please DO NOT include your personal telephone number on the title page.**

Abstract

Provide an informative 100 to 250 words abstract at the head of the manuscript. This should be a concise reflection of the aims, findings, conclusions and any interesting or important results. Carefully incorporate any terms that may be used by potential interested readers to improve the article's discoverability online (search engine optimisation). The abstract should contain no reference. Abbreviations that are not commonly used should be defined (for the benefit of the non-specialist reader) at first use.

Keywords

These are used for indexing. Please include between 3-5 keywords.

List of Notations

Please provide a list of symbols and definitions used in the text. This will ease our readers.

Introduction

A concise summary of current background knowledge, with reference to relevant previous works in the field should be presented. Please also describe the objectives of and justification for the work contained in the submitted manuscript.

Main Text

The methods and processes applied to investigate and achieve the objectives should be communicated in sufficient detail that readers could repeat the work successfully. The results should be reported clearly and interpreted accurately and analysed thoroughly. Figures/tables can be used to support these results.

It is important that all research articles include a section at the end of the main text that highlights the novelty of the results to the engineering field and any potential applications.

All sections should be numbered in Arabic such as 1, 2, etc. with the title in capitals. Sub-sections should be numbered such as 1.1, 2.3, etc. Numbered all equations in round brackets ( ) flush to the right. The equation should be in the centre.

Style for Illustrations (Tables and Figures)

Try to include the illustrations in between the text. Each illustration must be numbered such as "Figure 1, Figures 2-3, etc." and have a meaningful caption at the bottom. For tables, the caption must be at the top.
On graphs, show only the coordinate axes, or at most the major grid lines, to avoid a dense hard-thread result.

All lettering should be large enough to permit legible reduction of the figure to column width. Typing on figures is not acceptable. Photographs should be glossy prints, of good contrast and gradation and any reasonable size.

Conclusions

A concise summary of the results of case studies or research project papers and the lessons learned should be discussed. If necessary, please elaborate the applicability / relevance of your article to readers in other countries.

Research journals must discuss the practical relevance and potential applications of the engineering work described. This is important to readers working in engineering related practice.

Please also include relevant references to demonstrate how previous engineering research work has been used. These references could be standards, codes or relevant past journal papers.

Appendices

Additional information, such as tables or mathematical derivations can be included. These will be included in the article.

Acknowledgements

Please provide acknowledgement details to those persons or organization that contributed to the paper. Additional details required by funding bodies can be included.

References

The references to other literature that you have cited in your main text should be based on the APA style of referencing (Author, Date) as described below. Please refer https://apastyle.apa.org/ for a detailed guide on the referencing style.

- Single author: (Author, Year) or Author (Year)
- Two authors: (Author 1 & Author 2, Year) or Author 1 and Author 2 (Year)
- Three and more authors: (Author 1 et al., Year) or Author 1 et al. (Year)

In the text, the author and year of the reference should be put in parentheses immediately after the work referred to, for example 'Controlled tests on the Millennium Bridge (Chapman et al., 2005; Murray & Geddes, 1987; Wilby et al., 2011) during which…..' or 'as mentioned by Lim et al. (2018), the NCA derived from the agricultural wastes…'

All references must be listed, in full, at the end of the paper in alphabetical order, irrespective of where they are cited in the text.

In the reference section, the references should be written in full, as follows:

Books: Author 1 surname, author 1 initials, & Author 2 surname, author 2 initials. (Year of publication). Book title. Publisher, City, Country. doi reference. For example:

Kobayashi, K., Khairuddin, A. R., Ofori, G. & Ogunlana, S. (Eds.). (2009). *Joint ventures in construction*. Thomas Telford, London, UK.

Owen, G. & Totterdill, B. (2008). *The dispute board hearing. In Dispute Boards: Procedures and Practice*. Thomas Telford, London, UK.

Journal, magazine and newspaper articles: Author 1 surname, author 1 initials, & Author 2 surname, author 2 initials. (Year of publication). Paper title. Journal title, Volume (Issue number), First page-Last page. doi reference. Unpublished papers and theses should not be cited as they are not readily available.

Lim, J. L. G., Raman, S. N., Lai, F. C., Zain, M. F. M., & Hamid, R. (2018). Synthesis of nano cementitious additives from agricultural wastes for the production of sustainable concrete. *Journal of Cleaner Production*, 171, 1150-1160. https://doi.org/10.1016/j.jclepro.2017.09.143.

Soon, F. C., Khaw, H. Y., Chuah, J. H., & Kanesan, J. (2018). Hyper-parameters optimisation of deep CNN architecture for vehicle logo recognition. *IET Intelligent Transport System*, 12(8), 939-946. https://doi.org/10.1049/iet-its.2018.5127.

Conference proceedings: Author 1 surname, author 1 initials, & Author 2 surname, author 2 initials. (Year of publication). Paper title. Proceedings title, Volume (Issue number), First page-Last page. doi reference. Unpublished conference proceedings (i.e. that were only given to delegates) should not be cited as they are not generally available.

Chuah, J. H., Khaw, H. Y., Soon, F. C., & Chow, C. (2017). Detection of Gaussian noise and its level using deep convolutional neural network. *Proceedings of the TENCON 2017 - 2017 IEEE Region 10 Conference*, 2447-2450. https://doi.org/10.1109/TENCON.2017.8228272.

Unpublished material should not be included in the Reference list.

Please refer to https://apastyle.apa.org/ for a detailed guide on the referencing style. Authors should strictly adhere to the referencing style specified herein.

Mathematical Equations

Only relevant equations should be included in the main text and should be numbered. An equation editor program can be used to type in a formula.

Figures and tables caption list: Please supply a figure caption list at the end of your journal paper. Figures and tables must be put in the text in consecutive order. All figures must have a brief title accompanied with a short description.

Brief Profile

At the end of the manuscript, each author should provide a brief profile (less than 150 words), together with recent photographs (preferable less than 3 MB).

Corresponding Authors

We only permit one corresponding author per submission.

Conflict of Interest

Conflict of interest occurs when an author (or the author's institution) has personal or financial relationships that inappropriately influence the statements in the publication. Authors should ensure that publications will be written in an unbiased, ethical and responsible manner. The authors working on any sponsored engineering work or publications should declare such work under Conflict of Interest during submission.

Submission of Paper

Authors are required to submit via the IEM Online Journal Submission (OJS) through the following link:

https://iemjournal.com.my/index.php/iem/about/submissions.

Together with the manuscript, the corresponding author should enclose a cover letter containing the significance of the paper, the postal and email address, and telephone number for correspondence. In the cover letter, kindly provide four (4) names as reviewers. The selected reviewers must have the relevant knowledge and research experience. Provide the reviewers postal and email addresses and telephone numbers (if possible).

Further Enquiries

For further enquires, please contact Secretariat at the address shown below:

The Institution of Engineers, Malaysia
Bangunan Ingenieur, Lots 60 & 62, Jalan 52/4
Peti Surat 223 (Jalan Sultan), 46720 Petaling Jaya, Selangor Darul Ehsan
Tel: 03–78900130 Fax: 03–79577678
E-mail: pub@iem.org.my or iemjournal@gmail.com

The Institution of Engineers, Malaysia

Bangunan Ingenieur, Lots 60/62, Jalan 52/4, Peti Surat 223 (Jalan Sultan), 46720 Petaling Jaya, Selangor Darul Ehsan
Tel: 03-78900130 Fax: 03-79577678 E-mail: sec@iem.org.my IEM Homepage: http://www.myiem.org.my

REFEREES FOR VETTING OF IEM PUBLICATIONS

Dear IEM Members/Readers,

The Standing Committee on Information and Publications is revising the list of referees to assist in the vetting of articles received from members and non-members. The referees should preferably be at least Corporate Members of The Institution or graduates with higher degrees.

The aim of appointing the referee is to ensure and maintain a standard in the IEM Publications namely the bulletin and the Journal.

Members who are interested to be placed in the database of referees are to return the registration form to the IEM Secretariat, providing details of their degrees and particular expertise and experience in the engineering fields.

We need your services to look into the vetting of articles received for Publications and due acknowledgement would be announced yearly in the Bulletin. Referees must be committed to return the papers within a month from date of appointment.

Chairman
Standing Committee on Information and Publications

All correspondences are to be addressed to: -

The Chief Editor
Standing Committee on Information and Publications
The Institution of Engineers, Malaysia
Bangunan Ingenieur, Lots 60 & 62, Jalan 52/4
P.O. Box 223 (Jalan Sultan)
46720 Petaling Jaya
Selangor Darul Ehsan

Email: pub@iem.org.my

AREAS OF INTEREST FOR VETTING OF PAPERS

Please tick (√) the appropriate area of interest that you are able to vet the papers.

□ Acoustics
□ Engineering Education
□ Military Vehicles
□ Room Temperature
□ Aerodynamics
□ Environmental Engineering
□ Mini Pressure Meters
□ Safety Engineering
□ Air Conditioning
□ Fine Chemical
□ Mining Engineering
□ Scaffolding Works
□ Air Pollution Control
□ Finite Element
□ Naval Architecture
□ Seepage
□ Aircraft
□ Fire Detection
□ Navigation
□ Sewerage
□ Airport Engineering
□ Fire Engineering
□ Oil & Gas Engineering
□ Shipbuilding
□ Aluminium Design
□ Floods
□ Operation Research
□ Signal Processing
□ Arbitration
□ Food Processing

□ Palm Oil Industries
□ Solar Energy Technology
□ Automation
□ Foundation Engineering
□ Petrochemicals
□ Steelworks Design
□ Automotive Engineering
□ Fuzzy Logic
□ Petroleum Engineering
□ Stream Turbine Power Plant
□ Biochemical Engineering
□ Gas Engineering
□ Pharmaceuticals
□ Sructural Analysis
□ Biotechnology
□ Geotechnical
□ Piling
□ Structural Rehabilitation
□ Boiler Engineering
□ Heat Exchanger
□ Plumbing Engineering
□ Survey Engineering
□ Bridge Engineering
□ Highway
□ Pollution Control
□ Taligates
□ Building Services
□ Hydraulics
□ Ports & Harbour Engineering
□ Telecommunication

□ Coastal Engineering
□ H.V. Electrical Distribution
□ Power Electronics
□ Thermal Engineering
□ Co-Generation
□ Industrial Engineering
□ Power Generation
□ Timber Design
□ Computer Engineering
□ Industrial Transport
□ Pressure Vessels
□ Tool Engineering
□ Concrete Design
□ Industrial Ventilation
□ Prestressed Concrete
□ Transfer Tunnels
□ Concrete Technology
□ Information Technology
□ Project Management
□ Transportation Engineering
□ Construction Management
□ Instrumentation
□ Public Administration
□ Urban Planning
□ Control Engineering
□ Lighting System
□ Public Health Engineering
□ Vehicles
□ Drainage Engineering
□ L.V. Electrical Distribution

□ Quarry Engineering
□ Vertical Transportation
□ Dynamics Design
□ Manufacturing
□ Railways
□ Waste Treatment
□ Earthworks
□ Mass Transit
□ Reclamation Works
□ Waste Water
□ Edible Oil Refining
□ Mechanical Handling Equipment
□ Refrigeration
□ Water Resources Engineering
□ Electrical Transmission
□ Management
□ Reinforced Concrete Beams
□ Water Pollution Control
□ Electrochemical
□ Metal Fabrication
□ Road Transport
□ Wind Engineering
□ Electrotechnology
□ Metallurgy
□ Robotics
□ Others (please specify)
□ Energy Technology
□ Micro Electronics
□ Roof Structures

DISCIPLINES / SUB-DISCIPLINES OF VETTER

Please tick (√) the appropriate boxes.

□ Aerospace
□ Electrical
□ Marine
□ Petroleum

□ Aeronautical
□ Electronics
□ Mechanical
□ Production

□ Agricultural
□ Environmental
□ Mining
□ Structural

□ Chemical
□ Industrial
□ Naval Architecture
□ Others (Please specify)

VETTER'S DETAILS

Name : ____________________
Membership No. : ____________________ *(if applicable)*
Grade : □ Graduate □ Member □ Fellow □ Affliate □ Others
(please specify) ____________________
Qualifications : ____________________
Addresses : *(Office)* ____________________
____
(Residence) ____________________
____
Contact No. : __________ *(Handphone)* __________ *(Office)* __________ *(Residence)*
E-mail Address : ____________________

Please mail all correspondences to the below. Please tick (√) the appropriate boxes.
Mail to : □ Office □ Residence

Brief Biodata (not longer than 50 words) (to be appended with this Reply Slip).
____
____
____
____
____

Have you ever reviewed submissions for publication in any Journal(s) before? □ Yes □ No
If YES, name the Journal(s) ____________________

Do you have papers published in any Journal(s)? □ Yes □ No
If YES, name the Journal(s) ____________________

Date: __________ Signature : __________

IEM BRANCHES

PENANG	**IEM PENANG BRANCH SECRETARIAT** 1-04-02 E-Gate, Lebuh Tunku Kudin 2, 11700 Gelugor, Pulau Pinang	Tel : 04-606 599 iempenangbranch@gmail.com http://iempenang.org
SOUTHERN	**IEM SOUTHERN BRANCH SECRETARIAT** 24-B, Jalan Abiad, Taman Tebrau Jaya, 80400 Johor Bahru, Johor Darul Takzim	Tel : 07-331 9705 Fax : 07-331 9710 iemsouthern@gmail.com www.iemsb.org.my
PERAK	**IEM PERAK BRANCH SECRETARIAT** No. 60B, Jalan Lapangan Siber 1, Bandar Cyber (Business Centre), 31350 Ipoh, Perak Darul Ridzuan	Tel : 05-313 8459 iemperakbranch@gmail.com
EASTERN	**IEM PAHANG BRANCH SECRETARIAT** Ketua Penolong Pengarah Kanan Elektrik, JKR Cawangan Elektrik, Jalan Kamunting 2, Seri Kemunting, 25100 Kuantan, Pahang	Tel : 09-513 3533 Fax : 09-514 1594 mazman@jkr.gov.my
TERENGGANU	**IEM TERENGGANU BRANCH SECRETARIAT** 23-05, KT Business Centre, Padang Hiliran, Jalan Sultan Mohamad, 21100 Kuala Terengganu	Tel : 09-620 4500 Fax : 09-620 4502 iemterengganu@gmail.com
NEGERI SEMBILAN	**IEM NEGERI SEMBILAN BRANCH SECRETARIAT** No. 77-A-1, Lorong Haruan 5/3, Oakland Commerce Square, 70300 Seremban, Negeri Sembilan	Tel : 06-631 1011 Fax : 06-631 4619 iemnsembilan@gmail.com www.iemns.org.my
MELAKA	**IEM MELAKA BRANCH SECRETARIAT** C/O Sri Perunding Consulting Engineers, No. 2, Jalan Malinja 2, Taman Malinja Bukit Baru, 75150 Melaka	Tel : 06-284 8028 Fax : 06-283 8919 spcesb@gmail.com
SARAWAK	**IEM SARAWAK BRANCH SECRETARIAT** International Engineering Centre (IntEC), A2-G-19 & A2-1-19, Isthmus Raintree Square, Lot 3249, MTLD Block 7, Jalan Keruing, 93450 Kuching, Sarawak	Tel : 082-288 856 Fax : 082-288 856 iemsarawak@gmail.com
SABAH	**IEM SABAH BRANCH SECRETARIAT** Lot 25, 3rd Floor, Block C, Damai Point Commercial Centre, Lorong Damai Point, Off Jalan Damai, 88100 Kota Kinabalu, Sabah	Tel : 088-259 122 Fax : 088-236 749 iemsabah@gmail.com www.iemsabah.org.my
MIRI	**IEM MIRI BRANCH SECRETARIAT** 2nd Floor, Unit 14 (906-3-14), Soon Hup Tower Complex, (Mega Hotel), Jalan Merbau, 98000 Miri Sarawak	Tel : 085-423 718 Fax : 085-424 718 iem.miri@gmail.com www.iem-miri.org.my
KEDAH / PERLIS	**IEM KEDAH/PERLIS BRANCH SECRETARIAT** No. 164, Tingkat 2, Kompleks Alor Setar, Lebuhraya Darul Aman 05100 Alor Setar, Kedah Darul Aman	Tel : 04-734 3420 Fax : 04-733 3962 iemckps@gmail.com
PAHANG	**IEM PAHANG BRANCH SECRETARIAT** No. 114, Block F, Lorong Seri Teruntum, Medan Warisan, 25100 Kuantan, Pahang Darul Makmur	Tel : 019-855 6509 Fax : 09-514 6493 iempahang@gmail.com
KELANTAN	**IEM KELANTAN BRANCH SECRETARIAT** Lot 5139, Kompleks Niaga INOtrus Kawasan Perindustrian Pengkalan Chepa II, 6100 Kota Bharu, Kelantan	Tel : 09-773 0899 Fax : 04-733 3962 iemckps@gmail.com

THE INSTITUTION OF ENGINEERS, MALAYSIA
Bangunan Ingenieur, Lots 60 & 62, Jalan 52/4,
P.O. Box 223 (Jalan Sultan),
46720 Petaling Jaya, Selangor Darul Ehsan.

Tel: 03-7890 0130
Fax: 03-7957 7678
E-mail: sec@iem.org.my

www.myiem.org.my